Available online at www.sciencedirect.com
SCIENCE DIRECT®
Experimental Eye Research 81 (2005) 306–312
EXPERIMENTAL EYE RESEARCH
www.elsevier.com/locate/yexer

Transthyretin synthesis in rabbit ciliary pigment epithelium

Takahiro Kawaji[a], Yukio Ando[b,*], Masaaki Nakamura[b], Keiichi Yamamoto[b], Eiko Ando[a], Akiomi Takano[a], Yasuya Inomata[a], Akira Hirata[a], Hidenobu Tanihara[a]

[a]*Department of Ophthalmology and Visual Science, Graduate School of Medical Sciences, Kumamoto University, 1-1-1 Honjo, Kumamoto 860-8556, Japan*
[b]*Department of Diagnostic Medicine, Graduate School of Medical Sciences, Kumamoto University, 1-1-1 Honjo, Kumamoto 860-8556, Japan*

Received 1 August 2004; accepted in revised form 7 February 2005
Available online 9 March 2005

Abstract

Ocular symptoms of transthyretin (TTR)-related familial amyloidotic polyneuropathy (FAP) suggest that ciliary pigment epithelium (CPE) may synthesize TTR and its TTR may lead to amyloid formation in addition to TTR from vessels and retinal pigment epithelium (RPE). To clarify sites of TTR synthesis in ocular tissues, we performed in situ hybridization and reverse transcription-polymerase chain reaction (RT-PCR) for qualitative detection of TTR mRNA. In addition, we quantified levels of TTR mRNA expression by means of real-time quantitative RT-PCR. Furthermore, although TTR is an anti-acute phase protein in serum level, no reports on changes in TTR expression in ocular tissues during acute inflammation exist. To investigate changes in TTR expression in ocular tissues during inflammation, we induced uveitis by endotoxin challenge in rabbits and used real-time quantitative RT-PCR to examine changes in TTR mRNA expression in ocular tissues. In situ hybridization and RT-PCR qualitatively demonstrated TTR mRNA not only in RPE but also in CPE. Real-time quantitative RT-PCR showed that the level of TTR mRNA expression in the CPE was about one-third of that in the RPE. TTR mRNA expression in ocular tissues decreased as the degree of inflammation increased. These results suggest that TTR synthesized in the CPE may lead to ocular manifestations, especially glaucoma, in FAP. TTR mRNA also acts as an anti-acute phase reactant in ocular tissues.

Keywords: transthyretin; ciliary epithelium; familial amyloidotic polyneuropathy; glaucoma; anti-acute phase protein

1. Introduction

Transthyretin (TTR)-related familial amyloidotic polyneuropathy (FAP) is an autosomal dominant inherited disorder characterized by systemic accumulation of polymerized mutated TTR in the peripheral nerves and other organs, such as autonomic nervous system, choroid plexus, cardiovascular system, kidney, thyroid, gastrointestinal tract and eye (Ando et al., 1992). More than 100 different point mutations in the gene, most of which lead to production of amyloidogenic TTR (ATTR), have been identified in patients with FAP (Connors et al., 2003). In various types of FAP, ocular manifestations are commonly found although amyloid formation mechanism in ocular tissues as well as other systemic organs remains to be elucidated.

TTR is a 55-kDa tetramer protein in which each subunit is composed of 127 amino acids (Kanda et al., 1974). The main source of plasma TTR has been documented to be the liver (Felding and Fex, 1982), but the retinal pigment epithelium (RPE) (Martone et al., 1988; Cavallaro et al., 1990), the choroid plexus of the brain (Dickson et al., 1985; Soprano et al., 1985; Herbert et al., 1986) and the visceral yolk sac endoderm (Soprano et al., 1986) are also known to synthesize TTR. Furthermore, TTR protein had been detected in number of ocular tissues: RPE, retinal ganglion cells, nerve fiber layer of the retina, photoreceptor layer, ciliary epithelium, iris epithelium, lens capsule, corneal endothelium, and lacrimal glandular epithelium (Inada, 1988; Dwork et al., 1990). It plays an important role in plasma transport of thyroxin and, through its interaction with serum retinol-binding protein, of retinol (van Jaarsveld et al., 1973). The protein is an anti-acute phase protein whose serum levels decrease during acute inflammation, infection, and surgical stress. However, no reports on

* Corresponding author. Dr Yukio Ando, Department of Diagnostic Medicine, Graduate School of Medical Sciences, Kumamoto University, 1-1-1 Honjo, Kumamoto 860-8556, Japan.
E-mail address: yukio@kaiju.medic.kumamoto-u.ac.jp (Y. Ando).

0014-4835/$ - see front matter © 2005 Elsevier Ltd. All rights reserved.
doi:10.1016/j.exer.2005.02.003

changes in TTR expression in ocular tissues in such pathologic conditions exist.

Most FAP patients with secondary glaucoma have vitreous opacities, dandruff-like substances on the lens surface or pupillary margin, and pigment deposition in the chamber angle (Kimura et al., 2003). This evidence led to the common belief that ocular amyloid deposition originating from the vessels and the RPE may result in obstruction of the aqueous outflow route (Silva-Araujo et al., 1993). However, because we had observed several FAP patients who had glaucoma with severe amyloid deposition on the pupil and pupil fringe with little or no vitreous opacity (Futa et al., 1984), thus making this hypothesis less likely. TTR synthesized by sites other than the RPE in ocular tissues, sites close to the chamber angle, may predominantly cause glaucoma with amyloid deposition on the pupil and pupil fringe in such cases. We believed that one possibility would be additional TTR expression in ciliary pigment epithelium (CPE) cells, which, like the RPE cells, are differentiated from the outer layer of the embryologic optic cup.

In the present study, we clarified sites of TTR synthesis in ocular tissues in addition to the RPE and investigated the effect of inflammation on the change in TTR expression in ocular tissues by inducing uveitis in endotoxin-challenged rabbits.

2. Materials and methods

2.1. Animals

Japanese adult albino male rabbits (Kyudo Co., Kumamoto, Japan), 12 weeks of age and each weighing about 2·0–2·5 kg, were used in this study. The animals were treated in accordance with the ARVO Statement for the Use of Animals in Ophthalmic and Vision Research and the guidelines of the Committee on Animal Research of Kumamoto University.

2.2. Tissue preparation

The animals were killed by using an intravenously injected overdose of pentobarbital. Ten eyes were enucleated immediately and fixed overnight in a mixture of 4% paraformaldehyde in 0·1 M phosphate buffer at 4°C. The eyes were cut circumferentially at the cornea (2–3 mm anterior from the limbus) to remove the cornea and lens to make posterior cups, and samples were embedded in paraffin. These samples were used for in situ hybridization, reverse transcription-polymerase chain reaction (RT-PCR) analysis and real-time quantitative RT-PCR analysis. Forty eyes were cut circumferentially at the sclera (1 mm posterior from the limbus) to make anterior cups without RPE and posterior cups. CPE and RPE were obtained via dissection directly from anterior cups and posterior cups, respectively. These fresh tissues were frozen immediately with liquid nitrogen and stored at −80°C until use for real-time quantitative RT-PCR analysis.

2.3. Preparation of probes

Rabbit TTR cDNA samples were amplified by use of RT-PCR with rabbit liver mRNA, and cDNA was cloned into pDrive Cloning Vector (Qiagen, Tokyo, Japan). Plasmid templates were linearized, and fluorescein-substituted antisense and sense RNA probes were transcribed by using Fluorescein RNA Labeling Mix (Roche Diagnostics GmbH, Penzberg, Germany) and DIG RNA Labeling Mix (Roche Diagnostics GmbH), according to the manufacturer's protocols.

2.4. In situ hybridization

In situ hybridization was performed with a tyramide signal amplification system with fluorescein-labeled probes (GenPoint Fluorescein; Dako, Carpinteria) according to the manufacturer's instructions with a slight modification. Before hybridization, paraffin-embedded sections were immersed in three changes of xylene for 5 min. Residual xylene was removed by immersing the sections in two changes of 99% ethanol, followed by two changes of 95% ethanol, for each 3 min. Sections were then rehydrated with several changes of water and were pretreated with proteinase K (20 $\mu g\,mL^{-1}$) at room temperature (RT) for 10 min. After sections were washed with Tris–buffered saline/Tween (TBST), they were passed through a graded ethanol series (70, 95, and 99%). Hybridization in mRNA in situ hybridization solution (Dako, Carpinteria), containing 0·2 $\mu g\,mL^{-1}$ fluorescein-labeled RNA probes, which was preheated at 80°C, continued overnight at 45°C. After the sections were washed with the stringent wash solution twice at 55°C for 20 min and with TBST for 5 min, they were covered by 3% hydrogen peroxide at RT for 5 min. Samples were washed with TBST twice for 3 min, and then the antibody was incubated in anti-fluorescein isothiocyanate (FITC)-horseradish peroxidase (HRP) solution (×100 dilution) for 30 min at RT. After sections were washed three times with TBST for 3 min, they were covered by fluorescyl tyramide solution at RT for 15 min. Sections were washed again three times with the TBST for 3 min, and then anti-FITC-HRP solution was added to the sections at RT for 30 min. Sections were then washed three times with TBST for another 3 min, after which the sections were covered for 15 sec with 3,3′-diaminobenzidine chromogen with buffered solution containing hydrogen peroxide. The reaction was stopped by immersing the sections in water for 1 min. Sections were then viewed under the light microscope and photographed.

2.5. Isolation of RNA from targeted tissue areas and qualitative RT-PCR

To obtain pure CPE without RPE, we used the Pinpoint Slide RNA Isolation System II (Zymo Research, Orange) and isolated RNA from specific paraffin-embedded tissue areas on slides, according to the manufacturer's instructions.

RT-PCR was performed with SuperScript One-Step RT-PCR with Platinum Taq (Invitrogen, Carlsbad), according to the manufacturer's protocols. For the RT-PCR analysis, 1 μg of template RNA, 0·2 μM sense primers, 0·2 μM antisense primers, 1 μL of RT/Platinum Taq Mix, and 25 μL of 2× reaction mixture in a total volume of 50 μL were used. The primers were designed for spanning between exon 2 and exon 3 so that cDNA fragments were easily distinguishable from genomic fragments. RNA was reverse-transcribed into cDNA by one cycle at 50°C for 30 min followed by one cycle at 94°C for 2 min. The cDNA was amplified for 36 cycles: 94°C for 15 sec, 50°C for 30 sec, and 72°C for 1 min (the last cycle at 72°C for 5 min). After amplification, PCR products were run on 1·2% agarose gel, stained with ethidium bromide, and photographed with Printgraph (model AE-6911, ATTO, Tokyo, Japan), and the photographs were saved via Image Saver (model AE-6905, ATTO).

2.6. Real-time quantitative RT-PCR

Total RNA for analysis of TTR mRNA level on RPE cells and CPE cells was prepared from paraffin-embedded tissue samples by using Pinpoint Slide RNA Isolation System II and frozen tissue samples by using AquaPure RNA Isolation Kit (Bio-Rad, Hercules) according to the manufacturer's instructions. Total RNA for analysis of endotoxin-induced uveitis (EIU) model was prepared from frozen tissue samples by using AquaPure RNA Isolation Kit according to the manufacturer's instructions. The LightCycler RNA Master Hybridization Probe (Roche Diagnostics GmbH) is a specifically adapted product for one-step RT-PCR in glass capillaries using the LightCycler instrument and hybridization probes for detection. Real-time one-step PCR for TTR mRNA in rabbits was performed by using a LightCycler thermal cycling system according to the manufacturer's instructions. Glucose-6-phosphate dehydrogenase (G6PD) was used as internal control. The data for quantification were analysed with the LightCycler analysis software. TTR mRNA levels were estimated as the ratio of rabbit TTR mRNA copies to G6PD mRNA copies.

2.7. Generation of endotoxin-induced uveitis in rabbits

Lipopolysaccharide (LPS) from *Salmonella typhimurium* (Sigma, St Louis, MO) was dissolved in sterile phosphate-buffered saline (PBS) at a concentration of 1 mg mL^{-1}. Rabbits were anesthetized with intravenous pentobarbital (Nembutal; Dainippon Pharmaceuticals, Osaka, Japan) and intramuscular ketamine hydrochloride (Ketaral 50; Sankyo Pharmaceuticals, Tokyo, Japan). The pupils were dilated with a mixture of 0·5% tropicamide and 0·5% phenylephrine hydrochloride. A 30-gauge needle was inserted transconjunctivally at the temporal side (2–3 mm posterior to the limbus) with the aid of a surgical microscope. For each rabbit, 50 μg of LPS was injected into the vitreous cavity in one eye and 50 μL of PBS was administered to the other eye as the control.

Signs of uveitis were observed by slit lamp examinations at 3, 6, 12, 24, and 48 hr after LPS injection. The severity of the EIU was graded from 0 to 4 according to a previous definition (Ruiz-Moreno et al., 1992): 0, no inflammatory reaction; 1, discrete inflammatory reaction; 2, moderate dilation of the iris and conjunctival vessels; 3, intense iridal hyperemia with flare in the anterior chamber; and 4, same clinical signs as 3 plus presence of fibrinoid exudation in the papillary area with intense flare in the anterior chamber. Changes in TTR mRNA in the CPE and RPE were evaluated by real-time quantitative RT-PCR with the LightCycler system.

2.8. Statistical analysis

TTR mRNA levels are expressed as mean ± standard error of mean (S.E.M.). Differences were analysed via the paired *t*-test. Differences were considered significant when $P < 0{\cdot}05$.

3. Results

3.1. In situ hybridization

In situ hybridization assays of the rabbit eye sections with the antisense probe revealed the presence of hybridization signals for TTR mRNA not only within the RPE cells but also the CPE cells (Fig. 1A and C). The signals were distributed uniformly and abundantly within the cytoplasm of all RPE and CPE cells. Control sections hybridized with the sense probe showed no hybridization signal (Fig. 1B and D).

3.2. Isolation of RNA from targeted tissue areas and qualitative RT-PCR

We isolated RNA from specific paraffin-embedded tissue areas on slides (Fig. 2A). We applied the pinpoint solution on the targeted area with the aid of a microscope, which showed clearly that area 1 did not include RPE cells. RT-PCR revealed expression of TTR mRNA in CPE cells. The expression level in the RPE cells was higher than that in the CPE cells (Fig. 2B).

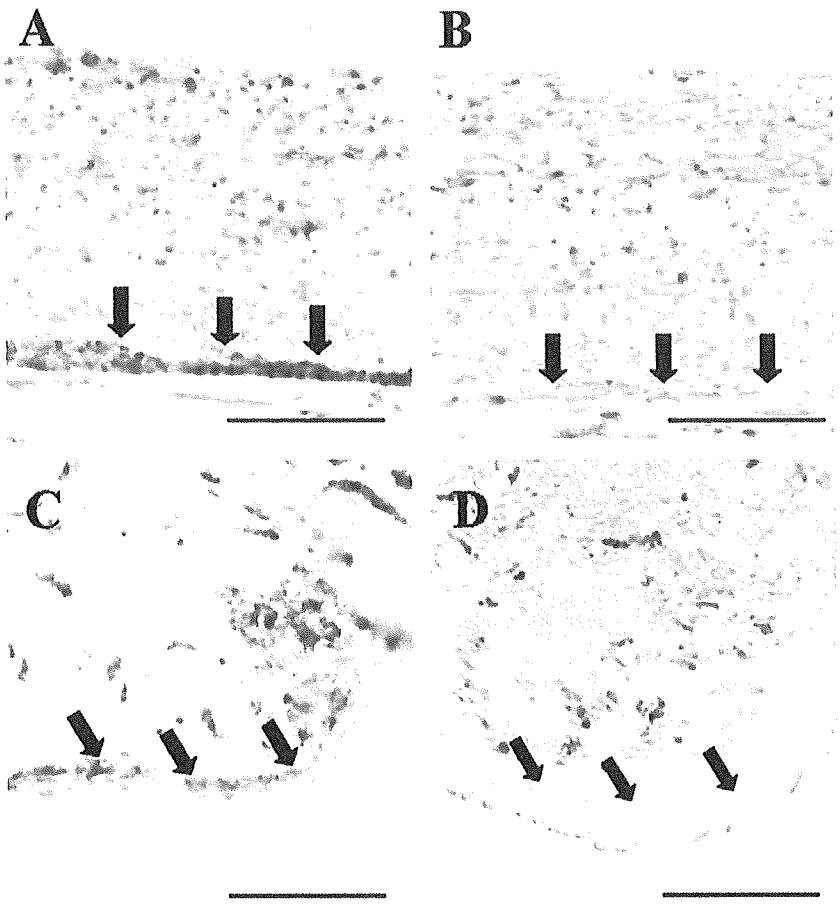

Fig. 1. In situ hybridization studies of rabbit eye sections via a tyramide signal amplification system with a fluorescein-labeled RNA probe for rabbit TTR. The tissues were analysed under light microscopy. Antisense (A) and sense (B) probes in RPE cells; antisense (C) and sense (D) probes in CPE cells. Bar represents 50 μm.

3.3. Real-time quantitative RT-PCR

Real-time quantitative RT-PCR analysis with the LightCycler revealed that the TTR mRNA level in CPE cells was approximately one-third of that in the RPE cells with both paraffin-embedded tissue samples and frozen tissue samples (Fig. 3).

3.4. Real-time quantitative RT-PCR with the EIU Model

Signs of uveitis, such as dilation of the iris and conjunctival vessels, iridial hyperemia, and flare in the anterior chamber, were discovered by means of slit lamp examinations 3 hr after intravitreous LPS injection, and the degree of change continued to increase up to 48 hr. Table 1 shows the time course of EIU grades after LPS injection. Control eyes had no signs of uveitis. Histological examinations showed that the number of inflammatory cells increased in iris and ciliary body, as compared to that seen in retina, in time-dependent manner (Fig. 4). Real-time quantitative RT-PCR analysis with the LightCycler revealed that TTR mRNA levels in the RPE cells decreased slightly until 6 hr after induction of inflammation (Fig. 5). However, at 12 hr and thereafter, TTR mRNA returned to normal levels. TTR mRNA levels in CPE cells were down-regulated by the induced inflammation.

4. Discussion

In this study, we presented new evidence of TTR production in CPE cells by means of qualitative and quantitative methods. In situ hybridization analysis of rabbit eyes revealed the presence of TTR mRNA not only in RPE cells but also in CPE cells. RT-PCR investigations demonstrated that RPE cells expressed higher TTR mRNA levels than did CPE cells. Real-time quantitative RT-PCR studies showed that the level of TTR mRNA expression in CPE cells was about one-third of that in RPE cells. After an inflammatory challenge achieved by intravitreous LPS injection, TTR mRNA levels in RPE cells decreased slightly until 6 hr after injection, but TTR mRNA levels in

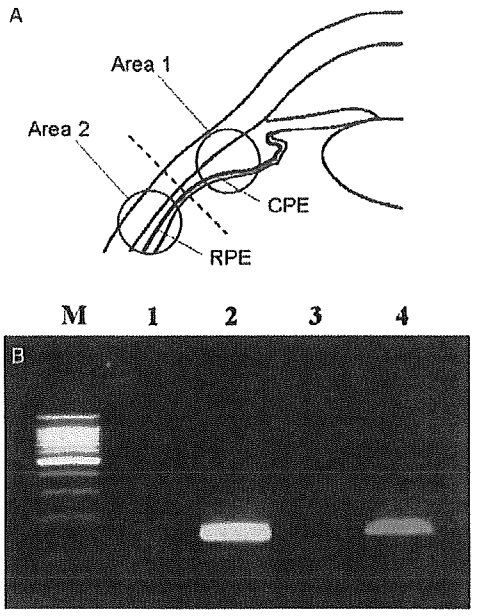

Fig. 2. RNA isolation areas in paraffin-embedded tissue and TTR expression as found in each area via RT-PCR. (A) Areas 1 and 2 included exclusively CPE cells and RPE cells, respectively. (B) Lanes 1 and 3, controls for RPE and CPE cells, respectively, reverse transcription (-); lane 2, RPE cells; lane 4, CPE cells; and lane M, size marker.

CPE cells were significantly down-regulated until 48 hr after injection. The grade of inflammation in around CPE cells was much higher than that in around RPE cells. These results suggest that TTR expression in RPE cells and CPE cells decreased as the degree of inflammation increased.

Our in situ hybridization analysis revealed TTR mRNA expression not only in RPE cells, as previously reported, but also in CPE cells, as we expected. Moreover, we isolated RNA from targeted tissue areas in which CPE cells were included and RPE cells were excluded by using the Pinpoint Slide RNA Isolation System II. Our RT-PCR analysis convincingly confirmed the presence of TTR mRNA expression in CPE cells.

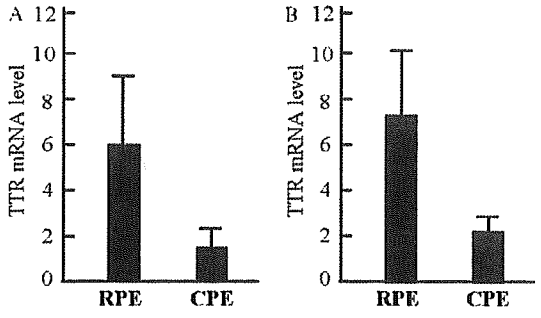

Fig. 3. Expression of TTR mRNA in RPE cells and CPE cells with paraffin-embedded tissue samples (A) and frozen tissue samples (B). The relative levels of mRNA expression were quantified and normalized to levels of G6PD mRNA expression. For each group in paraffin-embedded tissue samples, $n=4$. For each group in frozen tissue samples, $n=7$.

Table 1
Ocular inflammation after LPS injection

Time (hours after LPS injection)	EIU grade[a]
3	1.3
6	2.8
12	4.0
24	4.0
48	4.0

[a] Value represent the mean grade of EIU observed in five rabbits.

Cavallaro et al. (1990) first demonstrated by in situ hybridization methods that, in the rat eye, the RPE was the source of TTR synthesis and that an abrupt demarcation was present between hybridizing and nonhybridizing cells at the junction of the RPE and the CPE. The best possible explanation of the difference between their results and ours may be the sensitivity of the methodology: we used a tyramide signal amplification system with a fluorescein-labeled probe, whereas Cavallaro et al. used a ^{35}S-labeled probe and performed in situ hybridization alone. The sensitivity of the former is much higher than that of the latter (Tani, 1999). Another possibility is the fact that Cavallaro et al. studied rats and we studied rabbit, and that differences could be there purely because of the difference in animal model systems.

Quantitative analysis revealed significant production of TTR in CPE cells, with real-time quantitative RT-PCR demonstrating that the level of TTR mRNA expression in CPE cells was about one-third of that in RPE cells. These results suggest that a part of TTR in aqueous humor may be derived from CPE cells, and TTR synthesized by CPE cells may cause a part of amyloid deposition at the pupillary margin and angle chamber, which would result in glaucoma, while although we really do not know the source of TTR protein in aqueous humor. We accurately excised the tissues, and the reproducibility of the results of ISH and RT-PCR was reliable. Thus, our findings of TTR message in CPE cells does not invalidate our hypothesis that CPE cells is the main source of TTR in FAP patients who had secondary glaucoma with amyloid deposition on the pupil and pupil fringe but with little or no vitreous opacity. On the basis of our present studies, the mechanism of TTR delivery and release should be examined further.

As we described above, ISH and RT-PCR data and clinical evidence may support the contribution of CPE cells to form amyloid fibrils in the pupillary margin and angle chamber, however, ocular biochemical changes in rabbit is different from that in human. Therefore, same analysis should be performed in FAP patients and other animals.

Our study demonstrated that TTR mRNA levels in both CPE and RPE cells were regulated by acute inflammation in ocular tissues. As demonstrated in Fig. 4, the degree of inflammation increased in around CPE cells much higher than in around RPE cells in a time-dependent manner. In contrast, real-time quantitative RT-PCR clearly

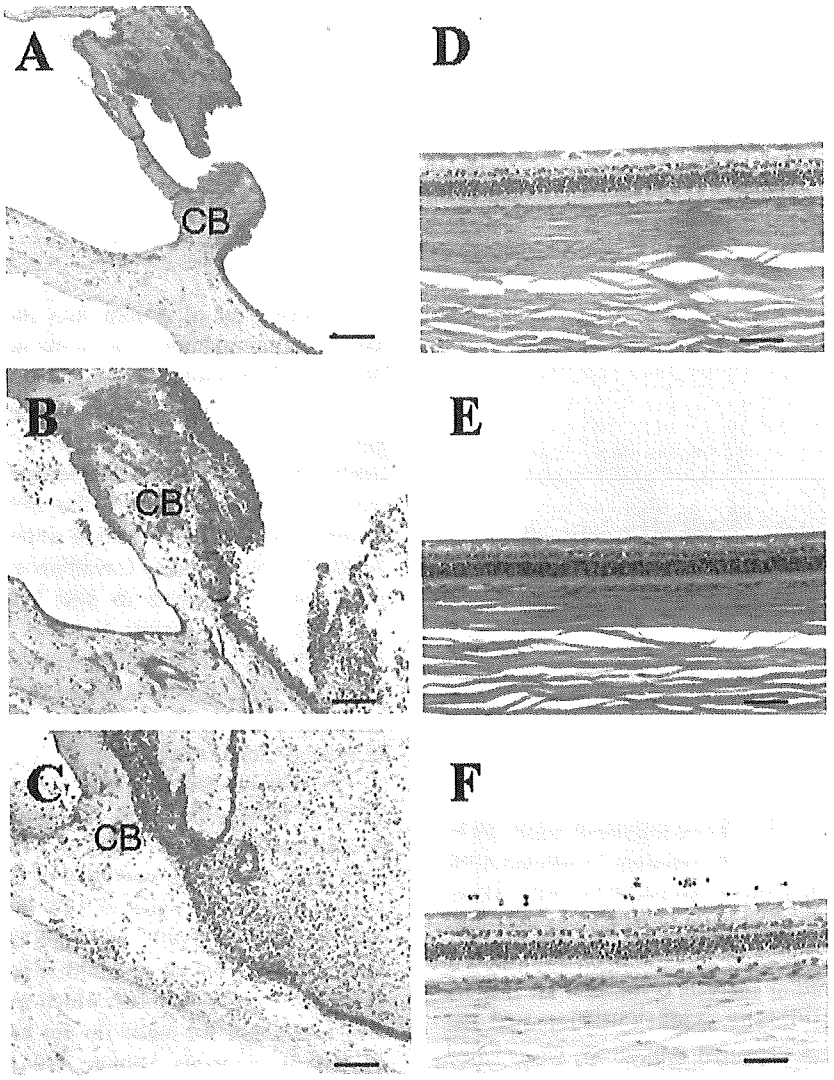

Fig. 4. Light-microscopic photographs of the HE-stained sections of the eyes at 6 (A, D), 12 (B, E) and 48 hr (C, F) after intravitreal LPS injection. Inflammatory cells in ciliary body (A, B, and C) increased much higher than that in retina (D, E, and F) in time-dependent manner. Bar represents 50 μm. CB, ciliary body.

demonstrated that TTR mRNA levels were suppressed, especially in CPE cells for much longer than in RPE cells, which suggests that TTR reacted as anti-acute phase protein in ocular tissues as well as in the liver.

Because TTR is predominantly synthesized by the liver, liver transplantation has been widely accepted as an effective therapy for halting amyloid deposition in systemic tissues (Holmgren et al., 1991; Ando et al., 1995). However, liver transplantation cannot prevent de novo amyloid deposition, and ocular manifestations continue to progress even after the surgery because of TTR synthesis in ocular tissues (Ando et al., 1996, 2000; Munar-Ques et al., 2000; Haraoka et al., 2002). As a result of longer follow-up periods and longer life expectancies of FAP patients, ocular manifestations, especially vitreous opacity and glaucoma, may become more frequent, serious complications for these patients after liver transplantation.

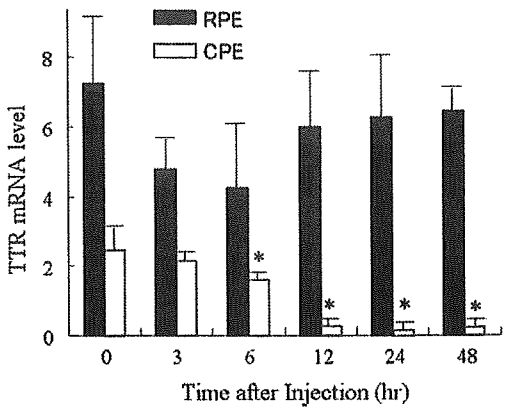

Fig. 5. Changes in TTR mRNA levels in RPE cells and CPE cells 0, 3, 6, 12, 24, and 48 hr after intravitreous LPS injection as described in the text. For each group, $n=5$. *$P<0{\cdot}05$, when compared to normal control (0 hr).

In conclusion, TTR is synthesized by CPE cells as well as RPE cells, whose production of TTR mRNA acts as an anti-acute phase reactant. TTR synthesized by CPE cells may lead to ocular manifestations, especially glaucoma in FAP patients.

Acknowledgements

The authors' work was supported by grants from the Amyloidosis Research Committee, the Pathogenesis, Therapy of Hereditary Neuropathy Research Committee, the Surveys and Research on Specific Disease, the Ministry of Health and Welfare of Japan, Charitable Trust Clinical Pathology Research Foundation of Japan, and Grants-in-Aid for Scientific Research (B) 15390275 from the Ministry of Education, Science, Sports and Culture of Japan.

References

Ando, Y., Araki, S., Shimoda, O., Kano, T., 1992. Role of autonomic nerve functions in patients with familial amyloidotic polyneuropathy as analyzed by laser Doppler flowmetry, capsule hydrograph, and cardiographic R–R interval. Muscle Nerve 15, 507–512.

Ando, Y., Tanaka, Y., Nakazato, M., Ericzon, B.G., Yamashita, T., Tashima, K., Sakashita, N., Suga, M., Uchino, M., Ando, M., 1995. Change in variant transthyretin levels in patients with familial amyloidotic polyneuropathy type I following liver transplantation. Biochem. Biophys. Res. Commun. 211, 354–358.

Ando, Y., Ando, E., Tanaka, Y., Yamashita, T., Tashima, K., Suga, M., Uchino, M., Negi, A., Ando, M., 1996. De novo amyloid synthesis in ocular tissue in familial amyloidotic polyneuropathy after liver transplantation. Transplantation 62, 1037–1038.

Ando, E., Ando, Y., Haraoka, K., 2001. Ocular amyloid involvement after liver transplantation for polyneuropathy. Ann. Intern. Med. 135, 931–932.

Cavallaro, T., Martone, R.L., Dwork, A.J., Schon, E.A., Herbert, J., 1990. The retinal pigment epithelium is the unique site of transthyretin synthesis in the rat eye. Invest. Ophthalmol. Vis. Sci. 31, 497–501.

Connors, L.H., Lim, A., Prokaeva, T., Roskens, V.A., Costello, C.E., 2003. Tabulation of human transthyretin (TTR) variants, 2003. Amyloid 10, 160–184.

Dickson, P.W., Howlett, G.J., Schreiber, G., 1985. Rat transthyretin (prealbumin). Molecular cloning, nucleotide sequence, and gene expression in liver and brain. J. Biol. Chem. 260, 8214–8219.

Dwork, A.J., Cavallaro, T., Martone, R.L., Goodman, D.S., Schon, E.A., Herbert, J., 1990. Distribution of transthyretin in the rat eye. Invest. Ophthalmol. Vis. Sci. 31, 489–496.

Felding, P., Fex, G., 1982. Cellular origin of prealbumin in the rat. Biochim. Biophys. Acta 716, 446–449.

Futa, R., Inada, K., Nakashima, H., Baba, H., Kojima, Y., Okamura, R., Araki, S., 1984. Familial amyloidotic polyneuropathy: ocular manifestations with clinicopathological observation. Jpn. J. Ophthalmol. 28, 289–298.

Haraoka, K., Ando, Y., Ando, E., Sun, X., Nakamura, M., Terazaki, H., Misumi, S., Tanoue, Y., Tajiri, T., Shoji, S., Ishizaki, T., Okabe, H., Tanihara, H., 2002. Presence of variant transthyretin in aqueous humor of a patient with familial amyloidotic polyneuropathy after liver transplantation. Amyloid 9, 247–251.

Herbert, J., Wilcox, J.N., Pham, K.T., Fremeau Jr., R.T., Zeviani, M., Dwork, A., Soprano, D.R., Makover, A., Goodman, D.S., Zimmerman, E.A., et al., 1986. Transthyretin: a choroid plexus-specific transport protein in human brain. The 1986 S. Weir Mitchell award. Neurology 36, 900–911.

Holmgren, G., Steen, L., Ekstedt, J., Groth, C.G., Ericzon, B.G., Eriksson, S., Andersen, O., Karlberg, I., Norden, G., Nakazato, M., et al., 1991. Biochemical effect of liver transplantation in two Swedish patients with familial amyloidotic polyneuropathy (FAP-met30). Clin. Genet. 40, 242–246.

Inada, K., 1988. Localization of prealbumin in human eye. Jpn. J. Ophthalmol. 32, 438–443.

Kanda, Y., Goodman, D.S., Canfield, R.E., Morgan, F.J., 1974. The amino acid sequence of human plasma prealbumin. J. Biol. Chem. 249, 6796–6805.

Kimura, A., Ando, E., Fukushima, M., Koga, T., Hirata, A., Arimura, K., Ando, Y., Negi, A., Tanihara, H., 2003. Secondary glaucoma in patients with familial amyloidotic polyneuropathy. Arch. Ophthalmol. 121, 351–356.

Martone, R.L., Schon, E.A., Goodman, D.S., Soprano, D.R., Herbert, J., 1988. Retinol-binding protein is synthesized in the mammalian eye. Biochem. Biophys. Res. Commun. 157, 1078–1084.

Munar-Ques, M., Salva-Ladaria, L., Mulet-Perera, P., Sole, M., Lopez-Andreu, F.R., Saraiva, M.J., 2000. Vitreous amyloidosis after liver transplantation in patients with familial amyloid polyneuropathy: ocular synthesis of mutant transthyretin. Amyloid 7, 266–269.

Ruiz-Moreno, J.M., Thillaye, B., de Kozak, Y., 1992. Retino-choroidal changes in endotoxin-induced uveitis in the rat. Ophthalmic Res. 24, 162–168.

Silva-Araujo, A.C., Tavares, M.A., Cotta, J.S., Castro-Correia, J.F., 1993. Aqueous outflow system in familial amyloidotic polyneuropathy portuguese type. Graefes Arch. Clin. Exp. Ophthalmol. 231, 131–135.

Soprano, D.R., Herbert, J., Soprano, K.J., Schon, E.A., Goodman, D.S., 1985. Demonstration of transthyretin mRNA in the brain and other extrahepatic tissues in the rat. J. Biol. Chem. 260, 11793–11798.

Soprano, D.R., Soprano, K.J., Goodman, D.S., 1986. Retinol-binding protein and transthyretin mRNA levels in visceral yolk sac and liver during fetal development in the rat. Proc. Natl Acad. Sci. USA 83, 7330–7334.

Tani, Y., 1999. PCR in situ amplification and catalyzed signal amplification: approaches of higher sensitive, non-radioactive in situ hybridization. Acta Histochem. Cytochem. 32, 261–270.

van Jaarsveld, P.P., Edelhoch, H., Goodman, D.S., Robbins, J., 1973. The interaction of human plasma retinol-binding protein and prealbumin. J. Biol. Chem. 248, 4698–4705.

Case II-2 of family 2 was a 90-year-old woman whose mother, children, and grandchildren were symptomatic patients with RP. She had no disturbance of night vision. Unfortunately, she could not visit our clinic to have a detailed assessment of her eyes.

The mutant mRNA was not expressed in the peripheral blood lymphocytes of Cases II-3, III-2, III-4, and III-5 in family 1. This finding suggested that the mutation induces functional loss of one allele resulting in haploinsufficiency.

The incomplete penetrance in RP11 could be attributable to the co-inheritance of a *PRPF31* gene defect and a low-expression of the wild-type allele.[6] Because a Chinese pedigree showed a high penetrance and a British family presented many asymptomatic carriers,[6,7] the expression of the wild-type allele of *PRPF31* gene may depend on the genetic background. To determine what genetic factors modulate the differential expression of the wild-type allele would be useful in the prognosis of family members with mutations.

In conclusion, we have identified two novel and one known mutations in three unrelated Japanese families with ADRP. This constitutes approximately 3% of the ADRP patients screened. There were also asymptomatic carriers in the Japanese population.

REFERENCES

1. Vithana EN, Abu-Safieh L, Allen MJ, et al. A human homolog of yeast pre-mRNA splicing gene, PRP31, underlies autosomal dominant retinitis pigmentosa on chromosome 19q13.4 (RP11). Mol Cell 2001;8:375–381.
2. Makarova OV, Makarova EM, Liu S, Vornlocher HP, Luhrmann R. Protein 61K, encoded by a gene (PRPF31) linked to autosomal dominant retinitis pigmentosa, is required for U4/U6+U5 tri-snRNP formation and pre-mRNA splicing. EMBO J 2002;21:1148–1157.
3. Kawamura M, Wada Y, Noda Y, et al. Novel 2336–2337delCT mutation in RP1 gene in a Japanese family with autosomal dominant retinitis pigmentosa. Am J Ophthalmol 2004;137:1137–1139.
4. Wada Y, Abe T, Takeshita T, Sato H, Yanashima K, Tamai M. Mutation of human retinal fascin gene (FSCN2) causes autosomal dominant retinitis pigmentosa. Invest Ophthalmol Vis Sci 2001;42:2395–2400.
5. Wada Y, Itabashi T, Sato H, Tamai M. Clinical features of a Japanese family with autosomal dominant retinitis pigmentosa associated with a Thr494Met mutation in the HPRP3 gene. Graefes Arch Clin Exp Ophthalmol 2004;242:956–961.
6. Vithana EN, Abu-Safieh L, Pelosini L, et al. Expression of PRPF31 mRNA in patients with autosomal dominant retinitis pigmentosa: a molecular clue for incomplete penetrance? Invest Ophthalmol Vis Sci 2003;44:4204–4209.
7. Wang L, Ribaudo M, Zhao K, et al. Novel deletion in the pre-mRNA splicing gene PRPF31 causes autosomal dominant retinitis pigmentosa in a large Chinese family. Am J Med Genet 2003;121:235–239.

Trans-Tenon Retrobulbar Triamcinolone Injection for Macular Edema Associated With Branch Retinal Vein Occlusion Remaining After Vitrectomy

Takahiro Kawaji, MD, Akira Hirata, MD, PhD, Nanako Awai, MD, Akiomi Takano, MD, Yasuya Inomata, MD, Mikiko Fukushima, MD, PhD, and Hidenobu Tanihara, MD, PhD

PURPOSE: To evaluate the effectiveness and safety of trans-Tenon retrobulbar triamcinolone injection for macular edema associated with branch retinal vein occlusion (BRVO) after vitrectomy.

DESIGN: Prospective interventional case series.

METHODS: The study included 20 eyes of 20 patients with BRVO, characterized by macular edema lasting more than 3 months after vitrectomy. Trans-Tenon retrobulbar injection of 40 mg triamcinolone was performed, and visual and anatomic responses were evaluated.

RESULTS: Mean foveal thickness was 499.4 ± 209.1 μm preoperatively, 281.8 ± 110.1 μm at 2-week follow-up, and 196.9 ± 92.1 μm at 6-month follow-up ($P < .0001$, at 2 weeks and 6 months, paired t test). Improvement of visual acuity by at least 0.2 logMAR (logarithm of the minimum angle of resolution) was seen in 14 (70%) of the 20 eyes.

CONCLUSIONS: Trans-Tenon retrobulbar injection of triamcinolone may be an alternative for additional treatment of eyes with BRVO that remains after vitrectomy.

RECENT INVESTIGATIONS HAVE DEMONSTRATED THE effectiveness of vitrectomy and its associated procedures for the decrease of macular edema in eyes with branch retinal vein occlusion (BRVO).[1] However, some cases of macular edema are resistant to vitrectomy. We evaluated the efficacy and safety of trans-Tenon retrobulbar triamcinolone injection for prolonged macular edema after vitrectomy in patients with BRVO.

Included in our study were 20 consecutive eyes of 20 patients with prolonged macular edema associated with BRVO lasting more than 3 months after vitrectomy.

Accepted for publication Feb 25, 2005.

From the Department of Ophthalmology and Visual Science, Graduate School of Medical Sciences, Kumamoto University, Kumamoto, Japan.

This study was supported in part by a Grant-in-Aid for Scientific Research from the Ministry of Education, Science, Sports and Culture, Japan, from the Ministry of Health and Welfare, Japan.

Inquiries to Hidenobu Tanihara, MD, PhD, Department of Ophthalmology and Visual Science, Graduate School of Medical Sciences, Kumamoto University, 1-1-1 Honjo, Kumamoto 860-8556, Japan; fax: (+81) 96-373-5249; e-mail: tanihara@pearl.ocn.ne.jp

TABLE 1. Baseline and Follow-up Data for 20 Patients Treated With Trans-Tenon Retrobulbar Triamcinolone Injection

Patient	Age (years)	Sex	Duration* (months)	Operation	Duration† (months)	Pre-VA	Final VA	Follow-up (months)	Recurrence
1	54	M	3	PEA + IOL + Vit (PVD)	10	0.1	0.4	14	+
2	68	M	26	PEA + IOL + Vit	9	0.08	0.04	14	–
3	78	F	3	PEA + IOL + Vit (PVD)	9	0.2	0.4	14	–
4	52	M	10	PEA + IOL + Vit (PVD)	7	0.1	0.3	13	–
5	50	F	1	Vit (PVD)	4	0.2	0.4	13	–
6	60	M	4	PEA + IOL + Vit (PVD)	21	0.2	0.5	13	–
7	84	F	3	Vit (PVD)	13	0.1	0.1	13	–
8	72	F	3	PEA + IOL + Vit (PVD)	3	0.2	0.4	13	–
9	69	M	2	Vit (PVD)	7	0.3	0.6	13	–
10	74	F	8	PEA + IOL + Vit (PVD)	13	0.1	0.3	12	–
11	73	M	26	PEA + IOL + Vit (PVD)	6	0.15	0.3	10	–
12	62	F	3	PEA + IOL + Vit	3	0.5	1	10	–
13	65	M	3	Vit (PVD)	4	0.3	0.4	7	–
14	67	F	4	PEA + IOL + vit (PVD, sheathotomy)	4	0.3	0.4	7	–
15	58	F	14	PEA + IOL + Vit (PVD, ILM)	10	0.3	0.6	6	–
16	79	F	2	PEA + IOL + Vit (PVD)	10	0.2	0.2	6	–
17	58	F	3	PEA + IOL + Vit (PVD, ILM)	3	0.3	0.4	10	–
18	61	M	9	PEA + IOL + Vit (PVD)	4	0.4	0.2	9	+
19	52	M	3	Vit (PVD)	5	0.1	0.2	8	–
20	59	F	7	PEA + IOL + Vit (PVD)	8	0.2	0.5	9	–

ILM = Peeling of the internal limiting membrane; IOL = intraocular lens implantation; PEA = phacoemulsification; PVD = surgical posterior vitreous detachment; VA = visual acuity; Vit = vitrectomy.

*Duration from onset of visual impairment to vitrectomy.

†Duration from vitrectomy to triamcinolone infusion.

Inclusion criteria were decimal best-corrected visual acuity of 0.5 or worse and foveal thickness greater than 250 μm. Trans-Tenon retrobulbar triamcinolone injection was performed as described previously.[2] Briefly, after topical anesthesia was administered, the conjunctiva and Tenon capsule were incised in the inferotemporal quadrant. A 23-gauge curved blunt cannula was then inserted into the sub-Tenon space, and 40 mg of triamcinolone acetonide was injected. Levofloxacin 0.5% was instilled four times daily for 1 week.

Data for all eyes are listed in Table 1. Mean ± SD duration between surgeries and triamcinolone injection was 7.7 ± 4.5 months (range 3 to 21). Mean follow-up period after injection was 10.7 ± 2.8 months (range 6 to 14). Mean foveal thickness was 499.4 ± 209.1 μm preoperatively, 281.8 ± 110.1 μm at 2-week follow-up, and 196.9 ± 92.1 μm at 6-month follow-up. Statistical analysis showed significant differences between preoperative and postoperative measurements ($P < .0001$ at 2 weeks and 6 months, paired t test). Visual acuity improved significantly from preoperative 0.74 ± 0.26 logMAR (logarithm of the minimum angle of resolution; range 1.1 to 0.3) to 0.46 ± 0.31 logMAR (range 1.0 to 0; $P < .0001$) at 6-month follow-up. Improvement of visual acuity by at least 0.20 logMAR was seen in 14 (70%) of 20 eyes. There were no eyes with visual loss of 0.20 logMAR or greater after injection. Fluorescein leakage area at late phase had decreased significantly at 1-month follow-up ($P = .0003$) from 10.5 ± 3.8 mm^2 (range 5.6 to 15.5) to 4.6 ± 2.6 mm^2 (range 2.6 to 7.7). Fluorescein leakage, which was evaluated subjectively in a masked fashion, in all eyes was improved. In two eyes, an additional injection was performed 3 and 6 months after the first because of recurrent macular edema. Intraocular pressure (IOP) elevation of 22 mm Hg or higher was found in seven (35%) of 20 eyes. IOP was controlled with antiglaucoma medications in all cases (Table 2). Cataract progression was noted in one of five phakic eyes.

Among the sequels to BRVO, macular edema directly affects the fovea and reduces visual acuity. Although vitreous surgeries are regarded as surgical modality for the treatment of macular edema, cases of macular edema do not always show anatomical or functional improvement in retinas after surgery. Recent clinical studies have shown that intravitreal injections of triamcinolone acetonide is effective for the treatment of macular edema.[3,4] However, intravitreal techniques carry the potential risks of vitreous hemorrhage, retinal detachment, and endophthalmitis,[5] as well as IOP elevation. Our results imply that in eyes even after vitrectomy,

TABLE 2. Summary of Changes in Foveal Thickness, Visual Acuity, and Intraocular Pressure*

Time Point	Foveal Thickness		logMAR Visual Acuity		IOP	
	Mean ± SD (μm)	*P* Value	Mean ± SD	*P* Value	Mean ± SD (mm Hg)	*P* Value
Baseline (n = 20)	499.4 ± 209.1	NA	0.74 ± 0.26	NA	12.2 ± 2.5	NA
2 weeks (n = 20)	263.5 ± 116.4	<.0001	0.49 ± 0.26	.0007	15.0 ± 4.2	.0004
1 month (n = 20)	231.8 ± 107.0	<.0001	0.48 ± 0.26	<.0001	15.8 ± 4.9	.0004
3 months (n = 20)	186.8 ± 67.7	<.0001	0.47 ± 0.28	<.0001	17.2 ± 7.1	.0018
6 months (n = 20)	192.5 ± 85.4	<.0001	0.46 ± 0.31	<.0001	15.1 ± 4.2	.0012
12 months (n = 10)	196.9 ± 92.1	.0116	0.51 ± 0.32	.0012	13.6 ± 3.0	.0772

IOP = Intraocular pressure; NA = not applicable.
*Differences were analyzed by the paired *t* test and considered significant when $P < .001$.

trans-Tenon retrobulbar injection of triamcinolone may be an alternative for additional treatment.

REFERENCES

1. Saika S, Tanaka T, Miyamoto T, Ohnishi Y. Surgical posterior vitreous detachment combined with gas/air tamponade for treating macular edema associated with branch retinal vein occlusion: retinal tomography and visual outcome. Graefes Arch Clin Exp Ophthalmol 2001;239:729–732.
2. Okada AA, Wakabayashi T, Morimura Y, et al. Trans-Tenon's retrobulbar triamcinolone injection for the treatment of uveitis. Br J Ophthalmol 2003;87:968–971.
3. Jonas JB, Sofker A. Intraocular injection of crystalline cortisone as adjunctive treatment of diabetic macular edema. Am J Ophthalmol 2001;132:425–427.
4. Gillies MC, Simpson JM, Billson FA, et al. Safety of an intravitreal injection of triamcinolone: results from a randomized clinical trial. Arch Ophthalmol 2004;122:336–340.
5. Moshfeghi DM, Kaiser PK, Scott IU, et al. Acute endophthalmitis following intravitreal triamcinolone acetonide injection. Am J Ophthalmol 2003;136:791–796.

Medial Canthal Tophus Associated With Gout

Yen Chang Chu, MD, Yi Yueh Hsieh, MD, and Lih Ma, MD

PURPOSE: To report a case with a gouty tophus at the medial canthus.

DESIGN: Observational case report.

METHODS: Review of the clinical, laboratory, photographic, and pathologic records of a patient with a gouty tophus at the medial canthus.

RESULTS: A 27-year-old man had a 3-year history of gouty arthritis and poorly controlled hyperuricemia. A medial canthal mass without discomfort developed gradually over 3 months. An excisional biopsy was performed, and the tissue was fixed in formalin for pathology. Analysis of a routine hematoxylin-and-eosin–stained section disclosed a multilobulated pseudocyst filled with amorphous eosinophilic material. Further staining with nonaqueous alcoholic eosin and viewed under a polarizing microscope indicated the presence of birefringent urate crystals.

CONCLUSIONS: Gouty tophus can develop progressively at the medial canthus, especially in people with uncontrolled hyperuricemia. A formalin-fixed specimen, stained with nonaqueous alcoholic eosin, demonstrates abundant birefringent urate crystals under a polarizing microscope. (Am J Ophthalmol 2005;140:542–544.

GOUT IS A COMMON RESULT OF VARIOUS DISORDERS that produce hyperuricemia. Deposition of urates in the joints may lead to recurrent attacks of arthritis. Tophi represent large aggregates of urate crystals and lead to inflammatory reactions. They are commonly seen in peripheral parts of the body but are rarely encountered by an ophthalmologist. We present a case with primary tophus formation at the medial canthus, which has not been reported in the literature.

A 27-year-old man came to our clinic for evaluation of a medial canthal mass in the right eye (Figure 1). The mass developed gradually over 3 months without discomfort. The patient denied previous trauma but had been diagnosed with gouty arthritis 3 years earlier. The arthritis involved only the proximal first metatarsal joint of the left foot. Because of recurrent attacks, the joint was mildly deformed. The patient did not control hyperuricemia regularly and only took medication during acute attacks. The concentration of serum uric acid was 10.4 mg/dl (normal range 3.8 to 7.0 mg/dL). Family history of hyperuricemia, but without gouty arthritis, was present in his mother and brother.

Accepted for publication Feb 25, 2005.

From the Departments of Ophthalmology (Y.C.C., L.M.) and Pathology (Y.Y.H.), Chang Gung Memorial Hospital, Taoyuan, Taiwan.

Inquiries to Lih Ma, MD, Department of Ophthalmology, Chang Gung Memorial Hospital, No. 5, Fu-Hsin Street, Kwei-Shan Shiang, Taoyuan, Taiwan; e-mail: malih1@adm.cgmh.org.tw

Available online at www.sciencedirect.com
SCIENCE DIRECT
ELSEVIER
Experimental Eye Research 82 (2006) 362–370
EXPERIMENTAL EYE RESEARCH
www.elsevier.com/locate/yexer

Rho-associated protein kinase inhibitor, Y-27632, induces alterations in adhesion, contraction and motility in cultured human trabecular meshwork cells

Tomoyo Koga[a], Takahisa Koga[a], Maiko Awai[a], Jun-ichiro Tsutsui[a], Beatrice Y.J.T. Yue[b], Hidenobu Tanihara[a,*]

[a]*Department of Ophthalmology & Visual Science, Kumamoto University Graduate School of Medical Sciences, Honjo 1-1-1, Kumamoto 860-8556, Japan*
[b]*Department of Ophthalmology and Visual Sciences, University of Illinois at Chicago, College of Medicine, USA*

Received 28 March 2005; accepted in revised form 11 July 2005
Available online 25 August 2005

Abstract

We investigated the roles of Rho-associated protein kinase (ROCK) in regulating activities such as adhesion, contraction and migration in cultured human trabecular meshwork (TM) cells. Human TM cells in culture were treated with Y-27632, a specific ROCK inhibitor. Trypan blue exclusion test and TUNEL staining showed little or no direct toxicity of Y-27632 on TM cells. By MTT assay, Y-27632 did not significantly affect the proliferation of TM cells. The cell adhesion assay showed that Y-27632 promoted the cell adhesiveness to both fibronectin and collagen type I in a dose-dependent manner. Collagen gel contraction activity of TM cells was significantly inhibited by the treatment of Y-27632 in a dose-dependent manner. The addition of Y-27632 accelerated motility of TM cells in wound healing assay. Phosphorylated LIM kinase 2 and cofilin, related to actin bundling and integrin clustering, were dephosphorylated (activated) by Y-27632. In conclusion, Y-27632 elicits profound effects on TM cell activities including adhesion, gel contraction, and cell motility. These Y-27632-induced changes of TM cells may be relevance to the physiology of the aqueous outflow system.

Keywords: Rho; ROCK; Y-27632; trabecular meshwork cells

1. Introduction

In human eyes, a majority (83–96%) of the aqueous humour leaves the eye through the trabecular meshwork (TM) and Schlemm's canal (conventional outflow) under physiologic conditions (Jocson and Sears, 1971; Bill and Phillips, 1971). Accumulating data have suggested that TM cells and their extracellular matrix (ECM) play important roles in regulating the conventional outflow pathway and the intraocular pressure (IOP). For instance, with aging, the aqueous outflow resistance increases while the number of TM cells decreases and the ECM composition in the juxtacanalicular region changes (Alvarado et al., 1981; McMenamin et al., 1986; Miyazaki et al., 1987). Fewer TM cells and abnormal deposition of the ECM have also been reported in glaucomatous eyes compared with normal eyes (Rohen, 1983; Alvarado et al., 1984; Alvarado et al., 1986; Knepper et al., 1996). It is believed that the outflow facility can be improved by modulating the TM cellular behaviour and that new IOP-lowering drugs may be designed through this process. So far, it has been reported that IOP can be reduced by cytoskeletal drugs such as cytochalasins (Kaufman and Barany, 1977; Kaufman and Erickson, 1982), ethacrynic acid (Epstein et al., 1987), a serine-threonine kinase inhibitor H-7 (Tian et al., 1998; Epstein et al., 1999), and protein kinase C inhibitor (Khurana et al., 2003).

Rho guanosine triphosphatase (GTPase), a member of the Rho subgroups of the Ras superfamily, participates in signalling pathways that play key roles in formation of actin stress fibres and focal adhesions, cytoskeletal rearrangements, cell morphology, cell motility and smooth muscle

Abbreviations effects of Y-27632 on human trabecular meshwork cells.

* Corresponding author. Hidenobu Tanihara, Department of Ophthalmology & Visual Science, Kumamoto University Graduate School of Medical Sciences, Honjo 1-1-1, Kumamoto 860-8556, Japan
E-mail address: tanihara@pearl.ocn.ne.jp (H. Tanihara).

0014-4835/$ - see front matter © 2005 Elsevier Ltd. All rights reserved.
doi:10.1016/j.exer.2005.07.006

contraction (Takai et al., 1995; Nobes and Hall, 1995; Kaibuchi et al., 1999). Recently, several putative target molecules of Rho have been identified as Rho effectors, including Rho-associated coiled coil-forming protein kinase named ROCK I (Nakagawa et al., 1996) (also known as p160 ROCK (Ishizaki et al., 1996)), and its isoform, ROCK II (Nakagawa et al., 1996) (also known as Rho kinase (Matsui et al., 1996) and ROK α (Leung et al., 1995)). ROCKs are important factors regulating focal adhesions and stress fibre formation in cultured fibroblasts and epithelial cells (Riento and Ridley, 2003). Y-27632 has been identified as a specific inhibitor of the ROCK/ROK family of protein kinases (Uehata et al., 1997). In a previous report from our laboratory, we noted that administration of this compound resulted in a significant reduction of IOP in rabbits in a dose-dependent manner (Honjo et al., 2001). We also demonstrated the presence of p160 ROCK in human TM cells and showed that ROCK inhibitors altered cell shape, disrupted actin bundles, and impaired focal adhesion formation (Honjo et al., 2001). Our studies along with others suggested that alterations in TM cellular behaviours might be the basis for the observed changes in the outflow facility (Tian et al., 2000; Lutjen-Drecoll et al., 2001; Rao et al., 2001).

Herein, we extended our effort in elucidating the physiology of the aqueous humour outflow by examining further the effects of Y-27632 on activities, including viability, proliferation, adhesion on the ECM, collagen gel contraction and motility of human TM cells in culture.

2. Materials and methods

2.1. Culture of human TM cells

Human eyes from donors aged 15, 22 and 47 years were obtained from the Illinois Eye Bank (Chicago). The procurement of tissues was approved by the Institutional Review Board at the University of Illinois at Chicago in compliance with the declaration of Helsinki. Trabecular tissues excised from eyes were cultured on Falcon Primaria flasks (Becton Dickson, Lincoln Park, NJ), as previously described (Yue et al., 1990; Sawaguchi et al., 1992; Zhou et al., 1996; Choi et al., 2005). The culture medium included Dulbecco's modified Eagle's medium (DMEM), 10% fetal bovine serum (FBS), and antibiotics. Cells were maintained at 37 °C in a 95% air −5% CO_2 incubator, and passaged using the trypsin-EDTA method. Human TM cells from passages 3 through 8 were used for subsequent studies.

2.2. Trypan blue exclusion test

The cytotoxicity of Y-27632 was evaluated using the trypan blue exclusion test. Viable cells were counted in vitro according to a previously described method (Jain et al., 1992). Briefly, 5×10^5 human TM cells were plated onto 100-mm dishes and grown for 24 hr. The medium was then replaced with fresh medium without or with Y-27632 (1, 10 and 100 μM). Twenty-four hour after the treatment, the cells were trypsinized and 1 mL of cell suspension containing 2×10^6 TM cells was prepared; 50 μL of 0.1% (vol/vol) trypan blue solution was then added to the cell suspension. Stained and unstained cells were counted by hemacytometer under a microscope 3 min after trypan blue treatment. The percentage of cell viability was calculated using the following formula: % cell viability = (viable cell count/total cell count) × 100. Five independent experiments were performed.

2.3. Terminal deoxyribonucleotidyl transferase (TdT)-mediated fluroscein-16-dUTP nick end-labelling (TUNEL) assay

Human TM cells plated on glass coverslips in 12-well culture plates were grown at 37 °C for 24 hr. Y-27632 (10 and 100 μM) was added and incubated for an additional 24 hr. The cells were then fixed with 4% paraformaldehyde in phosphate-buffered saline (PBS) for 15 min, washed with PBS, and permeabilized with 0.2% Triton X-100 for 5 min. For positive controls, the cells were incubated with 1 unit mL^{-1} DNase I (Invitrogen, Carlsbad, CA) for 10 min. TUNEL reaction was performed with Apoptosis Detection System, Fluorescein (Promega, Madison, WI) at 37 °C for 60 min according to the manufacture's protocol. After mounting using an anti-fade kit (Molecular Probes, Eugene, OR), the staining was observed under a fluorescence microscope (IX71, Olympus, Tokyo, Japan).

2.4. Cell proliferation assay

Proliferation of cultured human TM cells was measured by 3, (4,5-dimethyl-2-thiazolyl)-2,5-diphenylate-2Htetrazolium bromide (MTT), using a commercially available kit (Nacalai Tesque, Kyoto, Japan). Cells were plated in culture medium at a density of 1×10^4 cells per well in 96-well plates and allowed to adhere for 24 hr. After washing, the cultures were fed with fresh media, without or with Y-27632 (1, 10 and 100 μM) for 72 hr, and finally treated with 5 mg mL^{-1} MTT for 4 hr at 37 °C. The MTT solution was aspirated, and the formazan crystals were dissolved in detergent reagent for 10 min. The relative cell number was determined based on the optical absorbance of the formazan at 570 nm, using a control wavelength of 655 nm measured in automatic plate reader (BioRad, Hercules, CA).

2.5. Cell adhesion assay

Cell adhesion assay was conducted as previously described (Zhou et al., 1996). For the assay, the wells of 96-well plates were coated overnight with fibronectin (10 μg mL^{-1}) (Sigma, St. Louis, MO) or collagen type I (0.5 μg mL^{-1}) (Calbiochem, San Diego, CA) at 4 °C.

The remaining binding sites were blocked by 0.1% of bovine serum albumin (BSA) in PBS for 2 hr at room temperature. Human TM cells were suspended in culture medium containing 2 mg mL^{-1} of BSA without or with Y-27632 (at 10 or 100 μM), and were loaded ($n=4$) onto coated wells at 8×10^4 cells per well. After incubation for 60 min, the unattached cells were removed by aspiration. The remaining cells were fixed in 10% formalin and stained with 1% toluidine blue. They were then lysed and the intensity of the blue stain was measured with a microplate reader at 600 nm as an indication of cell density.

2.6. Immunocytochemical studies

TM cells were plated on glass coverslips in culture medium, and cultured overnight. Y-27632 at 100 μM was added for 60 min. After the drug exposure, the cells were fixed and permeabilized for 2 min in 3% paraformaldehyde-PBS with 5% Triton X-100 (Wako, Osaka, Japan), and were further fixed for 20 min with 3% paraformaldehyde. The samples were blocked in 2% BSA for 30 min. The coverslips were incubated for 60 min at room temperature with anti-β-catenin antibody (Sigma) diluted at 1:2000, or anti-pan-cadherin antibody (Abcam, Cambridgeshire, UK) diluted at 1:500 with blocking solutions. The samples were washed 3 times with PBS and incubated with Cy-3 conjugated anti-mouse secondary antibody (Jackson ImmunoResearch, West Grove, PA) or FITC conjugated anti-mouse secondary antibody (Jackson ImmunoResearch) for 30 min. After washing, the cells were mounted with anti-fade and observed by fluorescence microscope IX71.

2.7. Immunoblot analysis

Human TM cells (2×10^5 cells per well) were plated overnight in 6-well Falcon plates and were incubated with 10 or 100 μM of Y-27632 for 0.5 or 1 hr. Immediately after Y-27632 incubation or following a recovery period of 2 hr, the cells were gently washed with PBS and lysed in 500 μL of NuPAGE LDS sample buffer (Invitrogen) containing 0.05 M DTT (Invitrogen). The NuPAGE LDS sample buffer was commercially available, and consisted of 109 M Glycerol, 140.5 mM Tris, 106 mM Tris–HCl, 73 mM Lithium Dodesyl Sulfate, and 0.51 mM EDTA. After heating at 70 °C for 10 min in sample buffer, 15 μL of each sample was subjected to 4–12% NuPAGE Bis-Tris gel (Invitrogen) or 4–20% Tris-Glycine gel (Invitrogen) electrophoresis and transferred to nitrocellulose membrane (Protran, Schleicher and Schuell Bioscience, Keene, NH). The membrane was blocked for 60 min at room temperature in 5% skim milk and 0.1% Tween-20 diluted in Tris-buffered saline (TTBS) to minimize nonspecific immunoreaction. Some membranes were incubated for 1 hr at room temperature with anti-β-catenin antibody diluted at 1:4000, anti-pan-cadherin antibody diluted at 1:1000, anti-β-actin antibody (Ambion, Austin, TX) diluted at 1:500, or anti-glyceraldehyde 3-phosphate dehydrogenase (GAPDH) antibody (Biogenesis laboratories, Kommetjie, South Africa) diluted at 1:200 with dilution buffer (5% BSA in TTBS). Other membranes were subsequently incubated overnight at 4 °C with anti-phospho-LIM kinase 1/2 (Cell Signalling), anti-cofilin (Cell Signalling) or anti-phospho-cofilin (Cell Signalling) antibody diluted at 1:1000 with dilution buffer. The membrane was washed three times at room temperature for 10 min with TTBS. It was then incubated for 30 min at room temperature with horseradish-peroxidase-conjugated anti-mouse IgG antibody (1:500, Amersham Biosciences, Buckinghamshire, UK). After further washing, the membranes were incubated with enhanced chemiluminescence (Amersham Biosciences) and exposed to autoradiogram film to visualize immunoreactive bands.

2.8. Gel contraction assay

Collagen gel contraction assay was performed as previously described (Nakamura et al., 2002; Nakamura et al., 2003), with minor modifications. The wells of 24-well culture clusters were each coated at 37 °C with 1% BSA for 1 hr. Human TM cells were trypsinized and resuspended in culture medium at a density of 2.2×10^6 cells mL^{-1} without or with Y-27632 (1, 10 and 100 μM). Collagen type I (Nitta-gelatin, Osaka, Japan), 10×DMEM, reconstitution buffer (Nitta-gelatin), TM cell suspension and water were mixed in an ice bath at a ratio of 7:1:1:1:1 (final concentration of collagen type I, 1.9 mg mL^{-1}; final cell density, 2×10^5 cells mL^{-1}). The resultant mixture (0.5 mL) was added to each well of the BSA coated culture clusters, and collagen gel formation was induced by incubation at 37 °C for 90 min. DMEM (0.5 mL), without or with Y-27632 (1, 10 and 100 μM), was then added on top of the collagen gels. After 1 hr, the gels were freed from the walls of the culture wells with the use of a micro spatula. The diameter of the collagen gels was scanned into a computer and measured with a ruler every 24 hr for 3 days. The extent of contraction of the collagen gels mediated by the TM cells was expressed as decrease in gel diameter compared with the initial diameter.

2.9. Measurements of wound healing (cell motility) activities

Human TM cells were grown to confluence in 100-mm tissue culture dishes. Three or four sites in each dish were scraped from the confluent cells with a yellow plastic pipette tip to create a cleared line. The medium was removed and replaced with fresh medium without or with Y-27632 (10 and 100 μM). After incubation at 37 °C for 9 hr, the progress of cells moving into the wound area was photographed by microscope digital camera, DP70 (Olympus) and loaded into computer software, DP controller (Olympus). The shortest distance between the

edges of migrated TM cells (including its' protrusions) from both sides was measured by the ruler of this computer soft.

2.10. Stastical analysis

Data are presented as the mean ± S.D. and were statistically analysed by Student's *t*-test.

3. Results

3.1. Toxicologic experiments of Y-27632 on human TM cells

Trypan-blue exclusion test was performed to determine whether Y-27632 was toxic to TM cells. The percentage of the living TM cells without trypan blue staining was 99.7 ± 0.4% in control cultures without Y-27632 treatments ($n=5$). In experimental cultures treated with various concentrations of Y-27632, the percentages of trypan blue free (living) cells were between 99.4 and 99.6% ($n=5$), not statistically significant different from that in controls (Table 1). TUNEL staining was performed to investigate directly the effect on human TM cell death by the addition of Y27632. After treatments with DNase I, almost all of the TM cells became TUNEL-positive (Fig. 1). On the other hand, no TUNEL-positive cells could be detected even after 24 hr of Y-27632 treatment, although typical morphological changes were evident by light microscopy. Effects of Y-27632 on proliferation in cultured TM cells were evaluated with the use of MTT assay. No statistically significant differences between Y-27632 treated TM cells and controls could be discerned (Fig. 2). This inhibitor thus displayed little cytotoxicity and had no effect on the proliferative activity of TM cells.

3.2. Influence of Y-27632 on adhesion of TM cells onto ECM

To elucidate interactions between cultured human TM cells and ECM components, adhesion of TM cells onto

Table 1
Trypan blue exclusion test to evaluate cytotoxicity of Y27632 on cultured TM cells

	Exp. 1	Exp. 2	Exp. 3	Exp. 4	Exp. 5	Mean ± S.D.
TM (control)	100	100	100	99.2	99.3	99.7 ± 0.4
TM + Y27632 (1 μM)	98.9	99.1	100	100	99.4	99.4 ± 0.5
TM + Y27632 (10 μM)	100	99.1	100	100	98.9	99.6 ± 0.5
TM + Y27632 (100 μM)	99.1	100	100	99.1	100	99.6 ± 0.5

The percent of viable cells are shown. S.D., standard deviation; Exp, experiment.

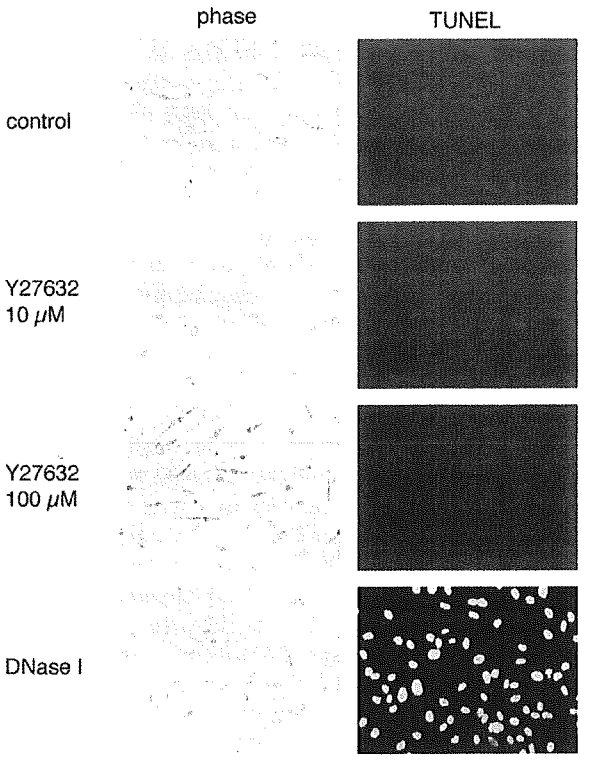

Fig. 1. Terminal deoxyribonucleotidyl transferase (TdT)- mediated fluroscein-16-dUTP nick end-labelling (TUNEL) staining on human TM cells without (control) or with the Y-27632 treatment for 24 hr. TUNEL positive cells were undetectable in TM cultures regardless whether they were untreated or treated with 10 μM or 100 μM Y-27632. In positive controls in which TM cultures were treated with DNase I, almost all of the cells were TUNEL positive (green).

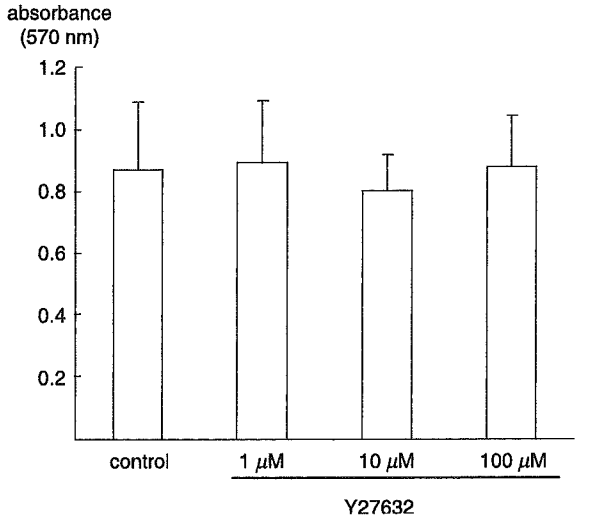

Fig. 2. Effect of Y-27632 on proliferation in human TM cells. Proliferation was measured by 3,(4,5-dimethyl-2-thiazolyl)-2,5-diphenylate-2H-tetrazolium bromide (MTT) assay. The data were expressed as the mean ± S.D. ($n=8$). Y-27632 did not affect human TM cell proliferation at any of concentrations (1, 10 or 100 μM).

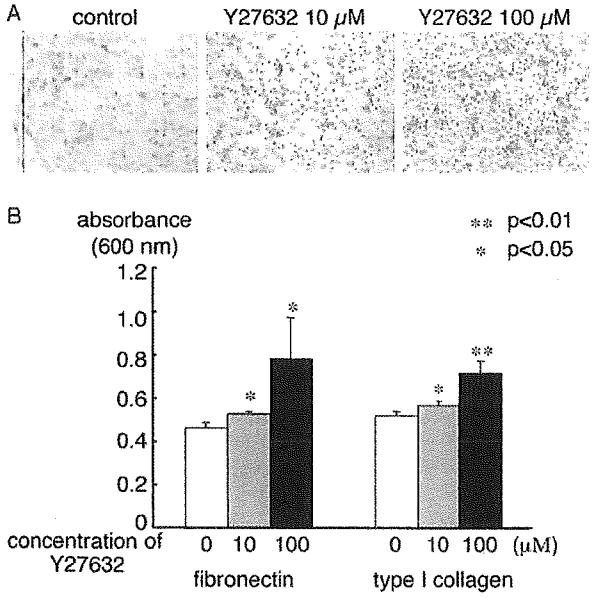

Fig. 3. Effect of Y-27632 on adhesion of human TM cells. Cells were plated on fibronectin (10 μg mL^{-1}) or collagen type I (0.5 μg mL^{-1}), and allowed to adhere in the absence or presence of Y-27632 (10 or 100 μM) for 60 min. The adhered cells were stained with 1% toluidine blue. The stained cells were lysed and the absorbance at 600 nm, a reflection of cell density, was measured. Data expressed as mean ± S.D. ($n=4$) were analysed by Student's t-test. The stained cells that were adhered on fibroectin are shown in A. Quantitative data are shown as bar graphs in B.

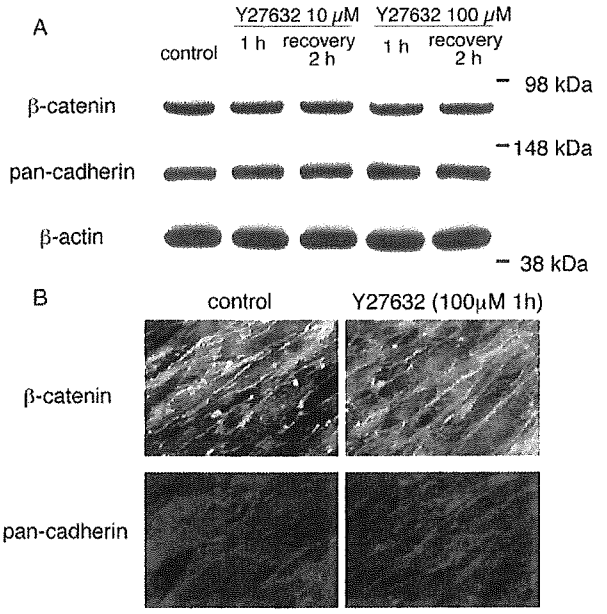

Fig. 4. (A) Level of β-catenin and pan-cadherin proteins in human TM cells treated with 0 (control), 10, or 100 μM of Y-27632. Immunoblot study was performed using lysates of cells collected immediately after Y-27632 treatment for 1 hr, or after incubation with fresh culture media without Y-27632 for an additional 2 hr (recovery 2 hr). (B) Distribution of β-catenin and pan-cadherin in human TM cells 1 hr after exposure to 100 μM of Y-27632. Experiments were repeated 3 times, yielding similar results.

fibronectin-coated or collagen type I-coated dishes was assayed. Compared with controls, a greater number of Y-27632-treated TM cells adhered onto fibronectin. Adhesion of TM cells to collagen type I was also increased by the addition of Y27632. The TM adhesion to both fibronectin and collagen type I was increased with increasing concentrations of Y-27632 (Fig. 3).

3.3. Effect of Y-27632 on cell–cell junction

In immunoblot analysis of cell–cell adhesion molecules, β-catenin (using anti-β-catenin antibody) and cadherins (using anti-pan-cadherin antibody) were detected under control medium without Y27632. These expression levels were not changed after Y27632 treatment for 1 hr and recovery for 2 hr. In immunocytochemical study, under control medium without Y27632, the cell–cell adhesions delineated by β-catenin and cadherins staining appeared as continuous or partially segmented lines along cell borders. After Y27632 treatment, these staining were also detected as continuous or partially segmented lines along borders of packed TM cells (Fig. 4).

3.4. Gel contraction assay

TM cells are known to induce contraction of collagen gel within which they are cultured (Nakamura et al., 2002; Nakamura et al., 2003). In our experiments, 24 hr after plating human TM cells with collagen gels, the change of the diameter of gels from the original value (16 mm) was 6.89 ± 0.38 mm ($n=3$). On the other hand, with 1, 10 and 100 μm Y-27632, the change of collagen gel diameter was 5.8 ± 0.8, 0.2 ± 0.4 and 0 mm (no detectable changes), respectively (Fig. 5). The results were statistically significant ($p<0.001$) and a dose dependency was evident. Similar results were also seen in experiments at 48 and 72 hr time points.

3.5. Wound healing (cell motility) activity of TM cells

Human TM cells in confluent cultures were scraped with a pipet tip to create cell-free wounds. At 9 hr after the scraping, the distance between the edges of exposed region was measured to be 75.0 ± 16.2, 28.1 ± 9.4 and 3.1 ± 5.4%, respectively, with Y-27632 at 0 (control), 10 and 100 μm (Fig. 6). The increase in the wound healing (cell motility) activity by Y-27632 was significant and concentration dependent.

In an effort to elucidate mechanisms related to actin remodelling and migration activities, we studied the status of phosphorylated forms of LIM kinase and cofilin. It has been reported that dephosphorylated LIM kinase leads to the dephosphorylated (active) form of cofilin, resulting in depolymerization of actin filament and promoting actin remodelling (Bamburg, 1999). Our immunoblot analysis showed that Y-27632 decreased the level of both

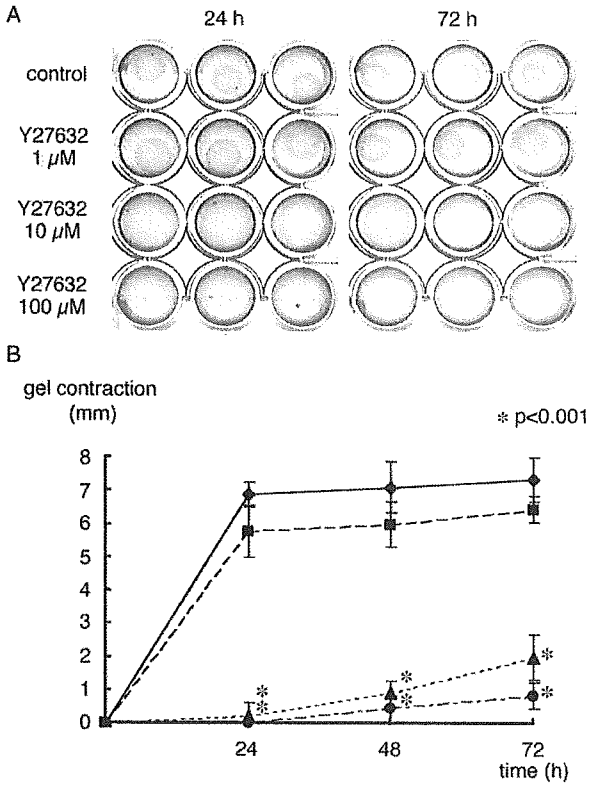

Fig. 5. Effect of Y-27632 on collagen gel contraction by human TM cells. (A) Collagen gels were incubated without (control) or with Y-27632 (1, 10 or 100 μM) for 24 or 72 hr. (B) The changes in diameter of collagen gels in the absence (◆, control) or presence of Y-27632 at 1 (■), 10 (▲) or 100 (●) μM were measured. Data shown as mean ± S.D. ($n=3$) were analysed by Student's t-tests. *$p<0.001$ versus control.

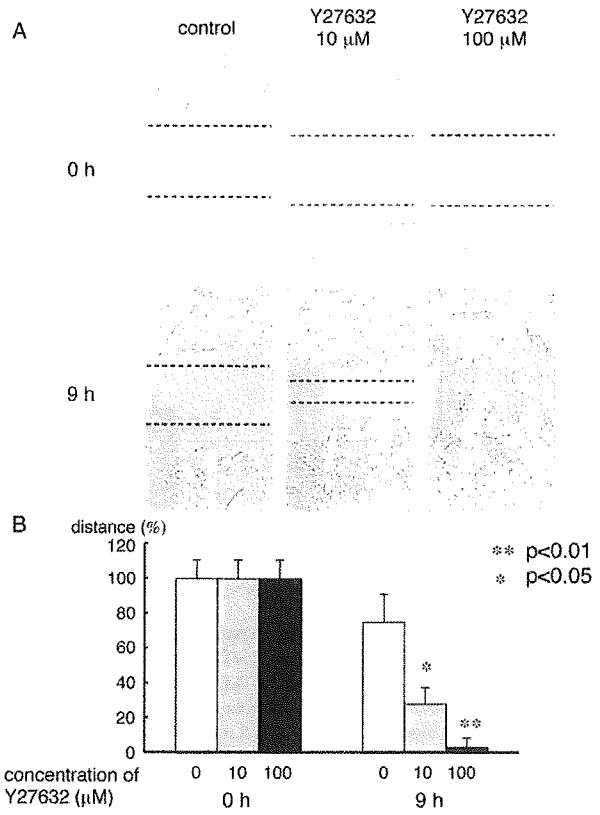

Fig. 6. Effect of Y-27632 on wound healing (motility) activities of human TM cells. (A) The cells grown to confluence were scraped with a yellow pipet tip to create a cell-free line. The medium was replaced with fresh medium without (control) or with 10 or 100 μM Y-27632. After 9 hr, migration of cells into the scraped area was photographed. The edges of migrated cells were indicated as dot lines. (B) The distances between the edges of migrated cells were measured, set at 100% before treatment, and shown as mean ± S.D. ($n=3$). Data were analysed by Student's t-test.

phosphorylated LIM kinase 2 and phosphorylated cofilin (Fig. 7). However, The level of phosphorylated LIM kinase 1 and total cofilin remained unaffected. The observed changes in the phosphorylated forms of LIM kinase 2 and cofilin were reversible after a 2-hr recovery period.

4. Discussion

The present study demonstrates that a specific inhibitor of the ROCK/ROK family of protein kinases, Y-27632, induces profound changes in various behaviours of cultured human TM cells. Exposure to Y-27632 results in cell retraction and rounding of cell bodies with protrusions. Despite these changes, Y-27632 is found not to be toxic. It does not induce cell death nor inhibit proliferation in TM cells.

Our results reveal that TM cellular adhesiveness to the ECM is enhanced by Y-27632. This finding is somewhat unexpected, since in our previous study (Honjo et al., 2001) a decreased focal adhesion formation and loss of actin stress fibres in TM cells were noted after treatment of this inhibitor. The actin cytoskeleton is known to interact with

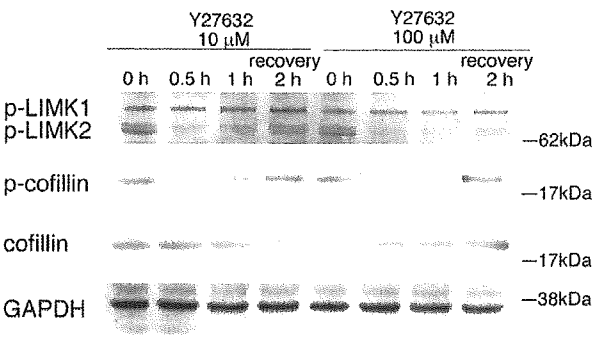

Fig. 7. Effects of Y-27632 on phosphorylation of LIM kinases and that of cofilin in human TM cells. Lysates were collected from cells untreated (control), or treated with 10 or 100 μM Y-27632 for 0.5 or 1 hr. Some dishes, after treatment of 10 or 100 μM Y-27632 for 1 hr, were incubated with fresh culture medium for an additional 2 hr (recovery 2 hr). Immunoblot analysis was performed for phosphorylated LIM kinase 1, phosphorylated LIM kinase 2, and phosphorylated and total cofilin. The levels of these proteins were normalized against that of GAPDH. Experiments were repeated 3 times, yielding similar results.

integrins to regulate cell shape and adhesiveness of cells to the matrix. In experiments using cultured THP-1 monocytes, inhibition of ROCK with Y-27632 did promote integrin adhesion that was accompanied by increases in membrane protrusions and phosphotyrosine signalling (Worthylake and Burridge, 2003). Similarly, in the present study, membrane protrusions were found in human TM cells after Y27632 treatment (data not shown). In addition, phosphotyrosine signalling and focal adhesion-associated molecules were concentrated at periphery of these protrusions by our immunocytochemical analysis (data not shown). The increased cell adhesiveness to ECM might be related to alterations in the cell shape and re-distribution of focal adhesions (and phosphotyrosine signalling) to the cell periphery.

Recent studies have indicated that cytoskeletal drugs including ROCK inhibitor decrease aqueous outflow resistance by destroying or stabilizing a complex of cytoplasmic fibres (Tian et al., 2000). Also, many cytoskeletal drugs have been reported to impair the adhesiveness of cell–cell or cell-matrix. For example, latrunculin-A was reported to be attenuated cell–cell attachments in human TM cells by immunocytochemical analysis (Cai et al., 2000). Protein kinase C inhibitor, which disrupt the actomyosin system, impair TM cell adhesion to ECM by quantitative adhesion assay (Zhou et al., 2000). In our study, protein expression level and distribution of cell–cell associated molecules such as β-catenin and pan-cadherin were almost unchanged after Y27632 treatment. Interestingly, adhesive activity to ECM was increased by the addition of Y27632. Decrease of the number of TM cells, that was observed in glaucomatous eyes, has been thought to be associated with decreased outflow facility and increased IOP (Rohen, 1983; Alvarado et al., 1984; Alvarado et al., 1986). The increased cellular adhesiveness to ECM by Y-27632 may prevent human TM cell decrease from TM tissues in glaucomatous eyes and can distinguish this inhibitor from other cytoskeletal drugs or inhibitors.

Contraction and relaxation of TM tissue are thought to control IOP (Thieme et al., 2000; Nakamura et al., 2002; Nakamura et al., 2003). In a previous study using bovine TM strips, Y27632 reduced TM tissue contraction (Thieme et al., 2000). In the present study, to investigate the direct effect of Y27632 on TM cellular contraction, we used three-dimensional cultures of human TM cells embedded in collagen type I gels. Gel contraction experiments reveal that addition of Y-27632 caused decreased contraction of collagen type I gel by TM cells. This phenomenon suggests reduced cell contractility and/or altered interaction between TM cells and collagen type I. However, as cell adhesion to collagen type I is found increased by addition of Y27632, the gel contraction change is thought to be due to just the TM cell relaxation by Y27632.

Administration of Y-27632, in addition, is shown to enhance motility of TM cells into the wound. This is in accordance with the notion that stabilization of actin stress fibres limits cell movement. Y-27632 also diminished the phosphorylation levels of LIM kinase 2 and cofilin. LIM kinase is the LIM domain-containing serine/threonine/tyrosine kinase composed of closely related LIM kinase 1 and LIM kinase 2 (Okano et al., 1995). They are known to be targets downstream of signalling by Rho GTPases. ROCK, specifically, has been shown to activate LIM kinase 2, but not LIM kinase 1 (Sumi et al., 2001). ROCK phosphorylates and activates LIM kinase 2, which phosphorylates and inactivates cofilin to suppress its actin-depolymerization and actin-severing activity, facilitating stress fibre formation (Bamburg, 1999). Consistent with this model, current experiments indicate that ROCK inhibitor Y-27632 reduces the levels of phosphorylated LIM kinase 2 and cofilin, not LIM kinase 1. The resulting dephosphorylated or active cofilin may in turn in TM cells promote actin depolymerization, formation of cell protrusions, and cell motility. These results suggest that the action of Y-27632 is, at least in part, mediated through the ROCK/LIM kinase 2/cofilin pathway. In previous reports, glucocorticoid, known to decrease aqueous outflow and cause secondary glaucoma, inhibits migration activities of TM cells (Clark et al., 1994). Furthermore, myocilin, known as a gene linked to both juvenile and adult-onset open angle glaucoma, also reduces migration activities of TM cells (Wentz-Hunter et al., 2004). In contrast, interestingly, our study revealed that Y-27632, an IOP lowering drug, accelerated migration activities of TM cells. Taken together, inhibition of migration activities might be associated with decreased aqueous outflow. However, further studies are required to reveal the association of migration activities and outflow facility.

In summary, the present study shows that Y-27632, a selective ROCK inhibitor, alters cellular behaviours of TM cells. It induces a reversible change in cell shape, increases cell adhesion, inhibits gel contraction, and accelerates cell migration. The IOP-lowering effect of Y-27632 observed in animal and perfusion organ culture studies (Honjo et al., 2001; Rao et al., 2001) is thus concluded to be related to the induced changes of TM cellular activities. Also, outflow facility was increased with gene transfer of dominant negative Rho A (Vittitow et al., 2002) or dominant negative binding domain of Rho-kinase (Rao et al., 2005) in anterior segments. The current data further specify that contractility in TM and/or Schlemm's canal cells may be a major factor in the physiology and regulation of the aqueous outflow, and that Rho/ROCK signal transduction is a key mediator of the cell contractility or relaxation. So far there have been accumulating data alluding to the usefulness of ROCK inhibitors as promising drugs in modulating the contractility of cells and lowering the IOP. The lack of toxicity of Y-27632, as demonstrated herein, offers an extra advantage in developing this inhibitor to be a therapeutic means for treatment of glaucoma.

Acknowledgements

This study was supported in part by a Grant-in-Aid for Scientific Research from the Ministry of Education, Science, Sports and Culture, Japan from the Ministry of Health and Welfare, Japan, and grants EY 05628 (BYJTY) and EY 01792 (core) from the National Eye Institute, Bethesda, MD, USA. The authors thank Professor Shuh Narumiya, Department of Pharmacology Kyoto University Faculty of Medicine for his kind advice.

References

Alvarado, J., Murphy, C., Polansky, J., Juster, R., 1981. Age-related changes in trabecular meshwork cellularity. Invest. Ophthalmol. Vis. Sci. 21, 714–727.

Alvarado, J., Murphy, C., Juster, R., 1984. Trabecular meshwork cellularity in primary open-angle glaucoma and nonglaucomatous normals. Ophthalmology 91, 564–579.

Alvarado, J.A., Yun, A.J., Murphy, C.G., 1986. Juxtacanalicular tissue in primary open angle glaucoma and in nonglaucomatous normals. Arch. Ophthalmol. 104, 1517–1528.

Bamburg, J.R., 1999. Proteins of the ADF/cofilin family: essential regulators of actin dynamics. Annu. Rev. Cell Dev. Biol. 15, 185–230.

Bill, A., Phillips, C.I., 1971. Uveoscleral drainage of aqueous humor in human eyes. Exp. Eye Res. 12, 275–281.

Cai, S., Liu, X., Glasser, A., Volberg, T., Filla, M., Geiger, B., Polansky, J.R., Kaufman, P.L., 2000. Effect of latrunculin-A on morphology and actin-associated adhesions of cultured human trabecular meshwork cells. Mol. Vis. 6, 32–43.

Choi, J., Miller, A.M., Nolan, M.J., Yue, B.Y.J.T., Thoz, S.T., Clark, A.F., Agarwal, N., Knepper, P.A., 2005. Soluble CD44 is cytotoxic to trabecular meshwork and retinal ganglion cells in vitro. Invest. Ophthalmol. Vis. Sci. 46, 214–222.

Clark, A.F., Wilson, K., McCartney, M.D., Miggans, S.T., Kunkle, M., Howe, W., 1994. Glucocorticoid-induced formation of cross-linked actin networks in cltured human trabecular meshwork cells. Invest. Ophthalmol. Vis. Sci. 35, 281–294.

Epstein, D.L., Freddo, T.F., Bassett-Chu, S., Chung, M., Karageuzian, L., 1987. Influence of ethacrynic acid on outflow facility in the monkey and calf eye. Invest. Ophthalmol. Vis. Sci. 28, 2067–2075.

Epstein, D.L., Rowlette, L.L., Roberts, B.C., 1999. Acto-myosin drug effects and aqueous outflow function. Invest. Ophthalmol. Vis. Sci. 40, 74–81.

Honjo, M., Tanihara, H., Inatani, M., Kido, N., Sawamura, T., Yue, B.Y.J.T., Narumiya, S., Honda, Y., 2001. Effects of Rho-associated protein kinase inhibitor Y-27632 on intraocular pressure and outflow facility. Invest. Ophthalmol. Vis. Sci. 42, 137–144.

Ishizaki, T., Maekawa, M., Fujisawa, K., Okawa, K., Iwamatsu, A., Fujita, A., Watanabe, N., Saito, Y., Kakizuka, A., Morii, N., Narumiya, S., 1996. The small GTP-binding protein Rho binds to and activates a 160 kDa Ser/Thr protein kinase homologous to myotonic dystrophy kinase. EMBO J. 15, 1885–1893.

Jain, P.T., Pento, J.T., Graves, D.C., 1992. Cell-growth quantitation methods for the evaluation of antiestrogens in human breast cancer cells in culture. J. Pharmacol. Toxicol. Methods 27, 203–207.

Jocson, V.L., Sears, M.L., 1971. Experimental aqueous perfusion in enucleated human eyes. Results after obstruction of Schlemm's canal. Arch. Ophthalmol. 86, 65–71.

Kaibuchi, K., Kuroda, S., Amano, M., 1999. Regulation of the cytoskeleton and cell adhesion by the Rho family GTPases in mammalian cells. Annu. Rev. Biochem. 68, 459–486.

Kaufman, P.L., Barany, E.H., 1977. Cytochalasin B reversibly increases outflow facility in the eye of the cynomolgus monkey. Invest. Ophthalmol. Vis. Sci. 16, 47–53.

Kaufman, P.L., Erickson, K.A., 1982. Cytochalasin B and D dose-outflow facility response relationships in the cynomolgus monkey. Invest. Ophthalmol. Vis. Sci. 23, 646–650.

Khurana, R.N., Deng, P.F., Epstein, D.L., Rao, P.V., 2003. The role of protein kinase C in modulation of aqueous humor outflow facility. Exp. Eye Res. 76, 39–47.

Knepper, P.A., Goossens, W., Hvizd, M., Palmberg, P.F., 1996. Glycosaminoglycans of the human trabecular meshwork in primary open-angle glaucoma. Invest. Ophthalmol. Vis. Sci. 37, 1360–1367.

Leung, T., Manser, E., Tan, L., Lim, L., 1995. A novel serine/threonine kinase binding the Ras-related RhoA GTPase which translocates the kinase to peripheral membranes. J. Biol. Chem. 270, 29051–29054.

Lutjen-Drecoll, E., Gabelt, B.T., Tian, B., Kaufman, P.L., 2001. Outflow of aqueous humor. J. Glaucoma. 10, S42–S44.

Matsui, T., Amano, M., Yamamoto, T., Chihara, K., Nakafuku, M., Ito, M., Nakano, T., Okawa, K., Iwamatsu, A., Kaibuchi, K., 1996. Rho-associated kinase, a novel serine/threonine kinase, as a putative target for small GTP binding protein Rho. EMBO J. 15, 2208–2216.

McMenamin, P.G., Lee, W.R., Aitken, D.A., 1986. Age-related changes in the human outflow apparatus. Ophthalmology 93, 194–209.

Miyazaki, M., Segawa, K., Urakawa, Y., 1987. Age-related changes in the trabecular meshwork of the normal human eye. Jpn. J. Ophthalmol. 31, 558–569.

Nakagawa, O., Fujisawa, K., Ishizaki, T., Saito, Y., Nakao, K., Narumiya, S., 1996. ROCK-I and ROCK-II, two isoforms of Rho-associated coiled-coil forming protein serine/threonine kinase in mice. FEBS Lett. 39, 189–193.

Nakamura, Y., Hirano, S., Suzuki, K., Seki, K., Sagara, T., Nishida, T., 2002. Signaling mechanism of TGF-β1-induced collagen contraction mediated by bovine trabecular meshwork cells. Invest. Ophthalmol. Vis. Sci. 43, 3465–3472.

Nakamura, Y., Sagara, T., Seki, K., Hirano, S., Nishida, T., 2003. Permissive effect of fibronectin on collagen gel contraction mediated by bovine trabecular meshwork cells. Invest. Ophthalmol. Vis. Sci. 44, 4331–4336.

Nobes, C.D., Hall, A., 1995. Rho, Rac and cdc42 GTPases: regulators of actin structures, cell adhesion and motility. Biochem. Soc. Trans. 23, 456–459.

Okano, I., Hiraoka, J., Otera, H., Nunoue, K., Ohashi, K., Iwashita, S., Hirai, M., Mizuno, K., 1995. Identification and characterization of a novel family of serine/threonine kinases containing two N-terminal LIM motifs. J. Biol. Chem. 270, 31321–31330.

Rao, P.V., Deng, P.F., Kumar, J., 2001. Epstein DL. Modulation of aqueous humor outflow facility by the Rho kinase-specific inhibitor Y-27632. Invest. Ophthalmol. Vis. Sci. 42, 1029–1037.

Rao, P.V., Deng, P., Maddala, R., Epstein, D.L., Li, C.Y., Shimokawa, H., 2005. Expression of dominant negative Rho-binding domain of Rho-kinase in organ cultured human eye anterior segments increases aqueous humor outflow. Mol Vis. 11, 288–297.

Riento, K., Ridley, A.J., 2003. ROCKs: multifunctional kinases in cell behavior. Nat. Rev. Mol. Cell Biol. 4, 446–456.

Rohen, J.W., 1983. Why is intraocular pressure elevated in chronic simple glaucoma? Anatomical considerations. Ophthalmology 90, 758–765.

Sawaguchi, S., Yue, B.Y.J.T., Chang, I.L., Wong, F., Higginbotham, E.J., 1992. Ascorbic acid modulates collagen type I gene expression by cells from an eye tissue-trabecular meshwork. Cell Mol. Biol. 38, 587–604.

Sumi, T., Matsumoto, K., Nakamura, T., 2001. Specific activation of LIM kinase 2 via phosphorylation of threonine 505 by ROCK, a Rho-dependent protein kinase. J. Biol. Chem. 276, 670–676.

Takai, Y., Sasaki, T., Tanaka, K., Nakanishi, H., 1995. Rho as a regulator of the cytoskeleton. Trends Biochem. Sci. 20, 227–231.

Thieme, H., Nuskovski, M., Nass, J.U., Pleyer, U., Strauss, O., Wiederholt, M., 2000. Mediation of calcium-Independent contraction in trabecular meshwork through protein kinase C and Rho-A. Invest. Ophthalmol. Vis. Sci. 41, 4240–4246.

Tian, B., Kaufman, P.L., Volberg, T., Gabelt, B.T., Geiger, B., 1998. H-7 disrupts the actin cytoskeleton and increases outflow facility. Arch. Ophthalmol. 116, 633–643.

Tian, B., Geiger, B., Epstein, D.L., Kaufman, P.L., 2000. Cytoskeletal involvement in the regulation of aqueous humor outflow. Invest. Ophthalmol. Vis. Sci. 41, 619–623.

Uehata, M., Ishizaki, T., Satoh, H., Ono, T., Kawahara, T., Morishita, T., Tamalawa, H., Yamagami, K., Inui, J., Maekawa, M., Narumiya, S., 1997. Calcium sensitization of smooth muscle mediated by a Rho-associated protein kinase in hypertension. Nature 389, 990–994.

Vittitow, J.L., Garg, R., Rowlette, L.L., Epstein, D.L., O'Brien, E.T., Borras, T., 2002. Gene transfer of dominant-negative RhoA increases outflow facility in perfused human anterior segment cultures. Mol Vis. 8, 32–44.

Wentz-Hunter, K., Kubota, R., Shen, X., Yue, B.Y.J.T., 2004. Extracellular myocilin affects activity of human trabecular meshwork cells. J. Cell Physiol. 200, 45–52.

Worthylake, R.A., Burridge, K., 2003. RhoA and ROCK promote migration by limiting membrane protrusions. J. Biol. Chem. 278, 13578–13584.

Yue, B.Y.J.T., Higginbotham, E.J., Chang, I.L., 1990. Ascorbic acid modulates the production of fibronectin and laminin by cells from an eye tissue-trabecular meshwork. Exp. Cell Res. 187, 65–68.

Zhou, L., Zhang, S.R., Yue, B.Y., 1996. Adhesion of human trabecular meshwork cells to extracellular matrix proteins. Roles and distribution of integrin receptors. Invest. Ophthalmol. Vis. Sci. 37, 104–113.

Zhou, L., Cheng, E.L., Rege, P., Yue, B.Y.J.T., 2000. Signal transduction mediated by adhesion of human trabecular meshwork cells to extracellular matrix. Exp. Eye Res. 70, 457–465.

Journal of Neurochemistry, 2006, **96**, 43–52 doi:10.1111/j.1471-4159.2005.03502.x

NMDA-induced retinal injury is mediated by an endoplasmic reticulum stress-related protein, CHOP/GADD153

Maiko Awai,*[,1] Takahisa Koga,*[,†,1] Yasuya Inomata,* Seiichi Oyadomari,† Tomomi Gotoh,† Masataka Mori† and Hidenobu Tanihara*

*Departments of *Ophthalmology and Visual Science and †Molecular Genetics, Kumamoto University Graduate School of Medical Sciences, Kumamoto, Japan*

Abstract

We investigated the role of an endoplasmic reticulum stress-associated protein, CHOP/GADD153, after NMDA-induced mouse retinal damage. After injection of NMDA into the vitreous, TUNEL-positive cells were detected in the retinal ganglion cell layer (GCL) and inner nuclear layer (INL) at 6 h after NMDA injection, and these gradually increased in number up to 24 h. Analysis by real-time RT-PCR revealed that CHOP mRNA was induced by about 3-fold, at 2 h after NMDA injection. Immunoreactivity for the CHOP protein was intense in cells of the GCL following NMDA treatment. Immunoblot analysis showed that NMDA injection increased the expression of CHOP protein in the retina. Compared with wild-type mice, $CHOP^{-/-}$ mice were more resistant to NMDA-induced retinal cell death as determined by TUNEL assay. At 7 days after NMDA treatment, the thickness of the inner plexiform layer and INL were larger in $CHOP^{-/-}$ mice than in wild-type mice. The number of residual cells in the GCL following NMDA treatment was significantly higher in $CHOP^{-/-}$ mice than in wild-type mice. In conclusion, CHOP is induced in mouse retina by NMDA treatment, and $CHOP^{-/-}$ mice are more resistant to NMDA-induced retinal damage, suggesting that CHOP plays an important role in NMDA-induced retinal cell death.

Keywords: C/EBP homologous protein, endoplasmic reticulum, NMDA, retinal ganglion cells.

J. Neurochem. (2006) **96,** 43–52.

Apoptotic cell death is associated with various retinal disorders, including human and experimental retinitis pigmentosa (Reme *et al.* 1998; Farrar *et al.* 2002), retinal ischaemia of animal model (Kuroiwa *et al.* 1998; Rosenbaum *et al.* 1998), and experimental glaucoma (Quigley *et al.* 1995) and human glaucoma (Kerrigan *et al.* 1997; Wax *et al.* 1998). Glutamate, an excitatory amino acid, causes retinal neuronal cell death. The *N*-methyl-D-aspartate (NMDA) receptor, which is one of the glutamate receptors, has been implicated in retinal neuronal cell death (Lam *et al.* 1999a). Administration of NMDA into animal vitreous cavities induced cell death in the ganglion cell layer (GCL) and inner nuclear layer (INL) of the retina (Joo *et al.* 1999). This retinal injury model has been widely used to investigate the mechanism of retinal neuronal cell death and to investigate neuroprotective factors and drugs (Inomata *et al.* 2003a,b).

The endoplasmic reticulum (ER) is an intracellular Ca^{2+} storage compartment in most cells. In the ER, newly synthesized 'secretary' proteins undergo glycosylation, disulfide bond formation, folding and oligomerization. These activities strictly depend on a high Ca^{2+} concentration in the ER (Alberts *et al.* 2002). Exposure of neurons to glutamate activates glutamate receptors and raises cytosolic Ca^{2+} levels.

Received April 21, 2005; revised manuscript received July 19, 2005; accepted August 22, 2005.

Address correspondence and reprint requests to Hidenobu Tanihara MD, Department of Ophthalmology, Kumamoto University School of Medicine, 1-1-1 Honjo, Kumamoto, 860–8556, Japan.
E-mail: tanihara@pearl.ocn.ne.jp

[1]These authors contributed equally to this work.

Abbreviations used: ARVO, Association for Research in Vision and Ophthalmology; ASK, apoptosis signal-regulating kinase; CHOP, C/EBP homologous protein; ECL, enhanced chemiluminescence; ER, endoplasmic reticulum; GADD153, growth arrest and DNA damage-inducible gene 153; GAPDH, glyceraldehyde-3-phosphate dehydrogenase; GCL, ganglion cell layer; HRP, horseradish peroxidase; INL, inner nuclear layer; NIH, National Institutes of Health; PAGE, polyacrylamide gel electrophoresis; PBS, phosphate-buffered saline; PI, propidium iodide; RGCs, retinal ganglion cells; SDS, sodium dodecyl sulfate; TBS, Tris-buffered saline; TSA, tyramide signal amplification; TUNEL, terminal deoxyribonucleotidyl transferase (TdT)-mediated fluroscein-16-dUTP nick-end labelling.

